USCIPI Report 760

A JOINT DETECTION-ESTIMATION APPROACH TO BOUNDARY ESTIMATION

by

Simon Lopez-Mora

June 1977

Image Processing Institute
University of Southern California
University Park
Los Angeles, California 90007

This research was supported by the Advanced Research Projects Agency of the Department of Defense and was monitored by the Wright Patterson Air Force Base under Contract No. F-33615-76-C-1203, ARPA Order No. 3119 and by the National Science Foundation in the form of a grant Contract No. ENG 75-03423.

UNCLASSIFIED

Security Classification

DOCUMENT CONTROL DATA - R & D

(Security classification of title, body of abstract and indexing annotation must be entered when the overall report is classified)

1. ORIGINATING ACTIVITY (Corporate author)

Image Processing Institute
University of Southern California, University Park
Los Angeles, California 90007

2a. REPORT SECURITY CLASSIFICATION

UNCLASSIFIED

2b. GROUP

3. REPORT TITLE

A JOINT DETECTION-ESTIMATION APPROACH TO BOUNDARY ESTIMATION

4. DESCRIPTIVE NOTES (Type of report and inclusive dates)

Technical Report, June 1977

5. AUTHOR(S) (First name, middle initial, last name)

Simon Lopez-Mora

6. REPORT DATE	7a. TOTAL NO. OF PAGES	7b. NO. OF REFS
June 1977	108	66

8a. CONTRACT OR GRANT NO.	9a. ORIGINATOR'S REPORT NUMBER(S)
F-33615-76-C-1203	USCIPI Report 760
b. PROJECT NO. ARPA Order No. 3119	
c.	9b. OTHER REPORT NO(S) (Any other numbers that may be assigned this report)
d.	

10. DISTRIBUTION STATEMENT

Approved for release: distribution unlimited

11. SUPPLEMENTARY NOTES	12. SPONSORING MILITARY ACTIVITY
	Advanced Research Projects Agency 1400 Wilson Boulevard Arlington, Virginia 22209

13. ABSTRACT

The estimation of object boundaries based on noisy observations is considered in the context of joint detection and estimation.

The images are expressed as replacement processes and the boundaries modeled in terms of geometrical parameters associated with the object. The images studied have two textures, object and background, characterized by their first and second order statistics. A boundary processor consisting of optima estimator and detector is derived, for an appropriately chosen cost function. Differences between the cost function and resultant processor with other costs and estimator-detector pairs used previously in other applications is indicated. The optimal solution involves a nonlinear estimator and a detector with a variable threshold dependent on the estimator output.

Further, because of information restrictions imposed on the estimator that alleviate its computational requirements, a recursive, easily implementable algorithm, updating only the first two moments is derived, and subsequently used to evaluate the estimate as well as to perform detection.

Experimental results are illustrated. Of particular significance is the applicability of said processor under very low signal to noise ratio conditions.

DD FORM 1 NOV 68 1473

UNCLASSIFIED

Security Classification

14. KEY WORDS	LINK A		LINK B		LINK C	
	ROLE	WT	ROLE	WT	ROLE	WT
Key Words: Boundary Estimation, Replacement Processes, Processor, Energy-Type Parameters, Hypothesis-Dependent Parameters, Joint Detection-Estimation.						

ACKNOWLEDGMENTS

I wish to express my sincere gratitude to Professor Nasser E. Nahi for his solicitous encouragement and guidance during the course of this research as well as for his courteous treatment, patience and financial support during my stay at USC.

I want to express my appreciation to the other members of my committee Professors David D. Sworder and Diane Schwartz.

I also want to thank the staff of the Image Processing Institute, in particular the former and present directors, Professors William K. Pratt and Harry C. Andrews, for their support, teaching and assistance during the past years.

Finally, I wish to thank Dr. Carlos A. Franco G., whose trust in me, made my presence at USC possible in the first place.

This research area supported in part by National Science Foundation Grant, ENG 75-Ø3423 and in part by the Advance Research Projects Agency of the Department of

Defence and was monitored by the Wright Patterson Air Force Base under Contract No. F-33615-76-C-1203.

TABLE OF CONTENTS

LIST OF FIGURES

ABSTRACT

The estimation of object boundaries based on noisy observations is considered in the context of joint detection and estimation.

The images are expressed as replacement processes and the boundaries modeled in terms of geometrical parameters associated with the object. The images studied have two textures, object and background, characterized by their first and second order statistics. A boundary processor consisting of optima estimator and detector is derived, for an appropriately chosen cost function. Differences between the cost function and resultant processor with other costs and estimator-detector pairs used previously in other applications is indicated. The optimal solution involves a nonlinear estimator and a detector with a variable threshold dependent on the estimator output.

Further, because of information restrictions imposed on the estimator that alleviate its computational requirements, a recursive, easily implementable algorithm, updating only the first two moments is derived, and subsequently used to evaluate the estimate as well as to

perform detection.

Experimental results are illustrated. Of particular significance is the applicability of said processor under very low signal to noise ratio conditions.

CHAPTER ONE

Segmentation is an important part of scene analysis. Image analysis or scene analysis is that branch of picture processing that deals with the determination of descriptions of pictorial data These descriptions (not necessarily pictorial) can indicate the types of regions or objects present in a scene, or their characteristics and interrelations. For instance the input can be a television image of a set of rocks while the output is a path on the terrain for a rover to move avoiding the obstacles (rocks). This evidently requires the determination of the location and size of the rocks. Or the input might be an aerial photograph of terrain while the desired output is a map showing specific types of terrain (reservoirs, forests urban areas, etc.). Here the output is pictoric also, but it requires the specification of the terrain type in addition to its location. As these descriptions are formulated in terms of parts (regions, objects curves, etc.) in the picture, it is clear that initially, the image needs to be segmented into these parts.

Digital pictures. in general. are represented by a 2-indexed function, s(i,j), whose values are indicative of

the amount of light reaching the observer from (i,j) and defined over a square grid of NxN points constituting the extent of the image. The value of this function at a point is referred to as the brightness, gray level or luminance of the picture at the point, while the points themselves are called picture elements or pixels.

Perhaps the oldest approach to segmentation is thresholding. By this method, the gray level differences are used to advantage in separating the regions of interest. For instance, given the image s(i,j), with luminance values in $[s_l, s_K]$ and containing, say, some objects on a darker background, then for an appropriately chosen threshold t, a new picture $s_t(i,j)$ can be derived:

$$s_t(i,j) = \begin{cases} 1 & \text{if} \quad s(i,j) \geq t \\ 0 & \text{if} \quad s(i,j) < t \end{cases} \qquad (1.1)$$

In $s_t(i,j)$ the desired objects are located at the non-zero pixel positions. The case of extracting dark objects from a brighter background can similarly be done. In fact, it may well be that the objects occupy a certain brightness range, thus, $s_t(i,j)$ can be defined as 1 for luminance values in such a range and zero elsewhere. This technique, however simple, presents several disadvantages resulting in part from the picture dependent threshold,

also the fact that in many applications the regions of interest may be characterized by other properties besides gray scale differences and most important, the fact that thresholding results deteriorate rapidly as the degradation (noise) in the original picture is more pronounced.

Several ways to alleviate these problems have been suggested [1]: they range from selection of a constant threshold so that a desired property of S_t is satisfied, to selection of variable thresholds throughout the picture [2], and also the use of preprocessing by a local property operator before thresholding [2,3].

A different alternative to image partitioning consists in determining the locations of abrupt changes in gray level. In monochrome pictures containing homogeneous (untextured) regions, edges form the boundaries between regions at different luminance values. Besides the step, other types of transitions (see Fig. (1.a)) are possible, e.g., roof, line, spike, etc. but only step edges will be considered, unless otherwise stated. The step edge previously indicated, however, is not present in normally available pictures. Several factors like point noise from the imaging system, reflections and object irregularities, and blurring effects between others, account for the appearance of edges like the one illustrated in Fig. (1.b). Maybe the simplest vertical edge detector is the one using

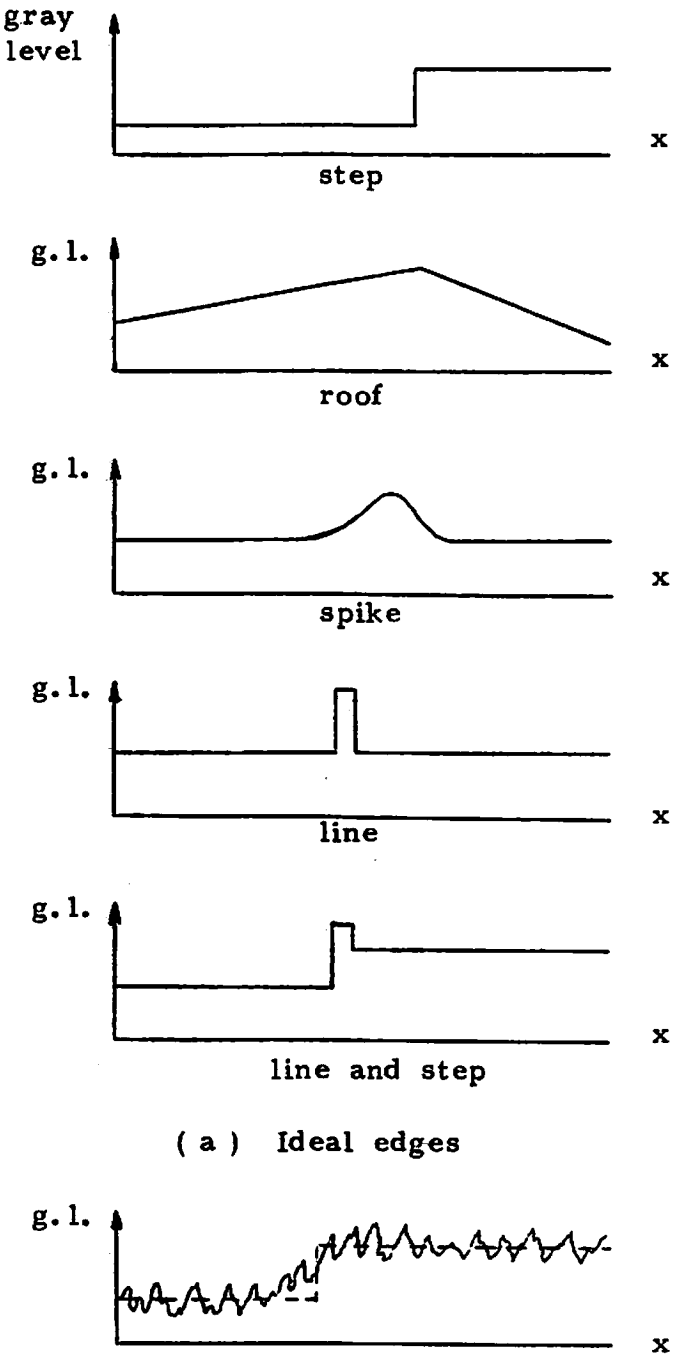

Fig. 1.1. Edge cross sections orthogonal to the edge direction.

$|s(i,j+1) - s(i,j)|$ i.e., the absolute value of gray level differences between pixels in adjacent columns and belonging to the same line. This edge detector associates an edge to (i,j) whenever the difference is large enough.

Related edge detectors are $[(s(i,j) - s(i+1,j+1))^2 + (s(i,j+1) - s(i+1,j))^2]^{\frac{1}{2}}$ proposed in [4] or the computationally simpler $|s(i,j) - s(i+1,j+1)| + |s(i,j+1) - s(i+1,j)|$, however these detectors are very sensitive to noise and surface irregularities mainly due to the small number of pixels (4) involved. In trying to overcome these difficulties, averaging based on bigger two-dimensional non-overlapping areas was proposed [5]. But as the neighborhood size increases, so does the amount of computations, besides, the transitions are now more gradual and the exact location of edges is unclear. Also it remains to specify the region size to use. References [5,6] indicate methods to lessen the effects of these problems. Edge detection (edges, lines, points) performed on 3X3 neighborhoods is carried out in [7]; in this approach a set of nine 3X3 orthonormal masks spanning the "edge" and "non-edge subspaces" is defined. Edges are accepted if a normalized projection onto the corresponding subspace is above a selected threshold i.e., the projection is close to one.

The edge detectors discussed up to this point have

been heuristic and dependent to a great extent on the extraction of the most prevalent features of edges: high derivatives and large values in the edge direction. In [8,9], however, the problem of best fitting an ideal edge to the picture gray levels is described. Reference [8] starts by defining an ideal edge as a function F on a circular disc D. Let

$$F(x,y,c,s,p,d,b) = \begin{cases} b & \text{if} \quad cx + sy \leq p \\ d + b & \text{if} \quad cx + sy > p \end{cases} \qquad (1.2)$$

with $c^2 + s^2 = 1$. The center of coordinates x-y coincides with the center of the disk. An empirical function E(x,y) continuous and constant over each grid square but arbitrary otherwise is also defined. The task of the operator is to best approximate a given empirical edge E with the ideal element F' so as to minimize

$$\int_D [E(x,y) - F(x,y,c,s,p,d,b)]^2 \, dx \, dy \quad . \qquad (1.3)$$

Instead of carrying out the minimization (1.3) directly, first a Fourier expansion of E and F in polar coordinates is performed, and then the resulting expression is truncated after eight terms. Let $\{H_i\}_{i=0}^{\infty}$ be the basis,

$$a_i(x, y) = \int_D H_i(x, y) \; E(x, y) \; dx \, dy \qquad (1.4)$$

$$s_i(x,y,c,s,p,d,b) = \int_D H_i(x, y) \; F(x,y,c,s,p,d,b) \; dx \, dy$$

$$\min \sum_{i=0}^{\ell} w_i [\, a_i(x, y) - s_i(x, y, c, s, p, d, b) \,]^2 \qquad (1.5)$$

with w_i representing weighting coeffients with values close to one. Truncation to only eight terms is justified because edges are usually blurred and blurring removes high spatial frequencies; also noise effects are more adverse at higher spatial frequencies. This operator returns the best edge and a measure of confidence on the fit.

For an optimal approach to line detection in the block world, see [10,11].

In regard to the edge detection approach to boundary detection, let us point out that results suffer from an excessive amount of edges not belonging to the boundary itself. This is not surprising in view of the local properties used in defining these detectors. In [12-14], boundary characteristics have been used to advantage in reducing the amount of redundant edges. Although the amount of edges is significantly lower, non-boundary edges are still present. Picture noise levels are a necessary consideration too. Edge detectors that discriminate edges very well in low noise, deteriorate considerably as the pictures become noisier [15,16]. A host of methods for boundary determination appear in [17,18,1], however their approach is via edge detection, hence they suffer from the

drawbacks previously adduced.

In addition to picture analysis, boundaries represent alternatives for data compression and image coding [19,20]. A different motivation, though, stems from the application of linear filtering techniques in picture restoration. To illustrate this point, consider for example the statistical representation of the image s(i,j) in terms of first and second order moments (a very common model for restoration). It was experimentally shown in [21] that, two-indexed, wide sense stationary random processes with exponential autocorrelations of the form

$$\mathrm{cov}[\,s(i,j)\,s(i+\ell,j+m)\,] = \mu\, e^{-\alpha|\ell|-\beta|m|} \qquad (1.6)$$

represent suitable models for the image s(i,j). Further use of (1.6) to derive linear dynamic models driven by white noise and the use of minimum mean square error criteria resulted in linear Kalman filters as restoration algorithms [22-26]. These filters represented real-time, recursive type procedures applicable even under non-stationarity assumptions. Wiener filters were also derived, on the other hand, by using second order statistics and the same error criteria [27,28]. However pictures restored by said methods consistently manifest a blurring of the edges.

To develop an understanding into the causes of this edge blurring, note first of all, that representing the image by its mean and autocorrelation functions, corresponds to aggregating the statistics from different picture entities, most importantly, textures, border lines and region geometries. Second, that the application of MMS criteria result in linear algorithms (the Wiener filter is certaintly one) that produce estimates at every pixel based on the whole picture data (or at least a big area) in general comprising several textures or regions. The direct effect of the latter point is a global smoothing of the data with the subsequent worsening of edge sharpness. Indeed, in representing images in terms of processes with statistics as in (1.6) (equivalently by using first and second order statistics), the geometric characteristics within the image have been undermined to such an extent that their recovery (estimation) is hampered. Hence, in accounting for the geometry, the model (1.6) is wanting. In remedying this condition, images were formulated in terms of "replacement processes" [29-31] (see also chapter two). These models bring up explicitly both picture aspects: texture and geometry. Early restoration results [32] showing better defined boundaries are supporting evidence of the available improvements obtained with the new formulation.

The first application of the replacement model to boundary estimation appeared in [29]. Said application involved an approximate maximum a posteriori (MAP) estimation of parameters representing the first and last lines where the object is present as well as the initial and final pixels delimiting the same between those lines. This recursive estimator suffered from several shortcomings, the most prominent involving the ad hoc estipulation of variances in crucial transition densities of the initial and final pixels in lines occupied by the object. Further, it has application to pictures with only one object (there is one initial line and one final line).

More recently, preliminary results obtained in [33] with a MMS estimator for boundaries in pictures represented in terms of replacement processes, unveiled a new approach for boundary determination which will be the subject of this dissertation. Unlike [33] where ad hoc procedures of boundary rejection were necessary, this new approach accounts in an optimal manner for the absence of the object at any line. In addition, the algorithm is not constrained to process one-object pictures. Of particular interest are its recursive on-line operation, use of only first and second order statistics and ability to operate under severe noise environments.

The following is an outline of the succeeding pages:

In chapter two, the subject of boundary estimation in the context of the replacement formulation is taken up. When the images are two-textured and contain horizontally convex objects, the boundary function (process) is shown to be advantageously expressed in terms of two parameters with clear geometric meaning: width and center. The images considered are characterized statistically in terms of the first and second statistics of the textures, the noise degradation and the width and center statistics (Markovian sequences).

Chapter three elaborates on the type of structure necessary to perform boundary estimation and finds the optima detector and estimator that minimize the average cost of joint detection and estimation for a desired cost function. Furthermore, estimation and detection algorithms, recursive, easily implementable, updating only first and second order moments are developed.

The processing of binary pictures and experimental results are presented in detail in chapter four.

Finally, chapter five discusses other possible algorithms, the use of different cost functions and topics for further research.

CHAPTER TWO

Problem Formulation

Pictures are subject to many different types of degradations, stemming from camera motion, out-of-focus imagery, atmospheric turbulence, background radiation, quantization, to name a few. As a result, in practice, the original gray level values of an image, s(j,m), are unavailable for measurement. Instead of s(j,m), a degraded form (the observable image), y(j,m), hereafter called the "observation," is available. Many times, the original is corrupted by some type of noise. Some of these are uncorrelated from point to point, others are not (noise due to the presence of TV raster lines); some are independent of the picture signal (channel noise introduced during transmission, scanning noise from a vidicon television camera), while others are not (photographic graininess, flying spot scanning noise)[1]. In this work, we will be concerned with the more common types of distortions, namely, those modelled by additive noise.

On the planar grid (double-indexed) where the observations y(j,m), j,m=1,...,N are defined, it is possible to assign also a temporal ordering, k. For a

picture already available, this latter ordering might be artificial. On the other hand, it can be indicative of the image generation, i.e., the successive availability of the elements in the sequence of observations.

Ordinarily, when an image scanner is used, the temporal order indicated by k is directly related to the scanning process. In the following, a line by line scanning will be assumed, left to right and from top to bottom. Hence, the ordering rule becomes:

$$\begin{aligned} k &= (j-1)N + m \\ j &= 1,\ldots,N \\ m &= 1,\ldots,N \\ k &= 1,\ldots,N^2. \end{aligned} \qquad (2.1)$$

The images that will be dealt with are all expressed in terms of replacement processes.

Replacement Processes : In its general form (in the image context), a replacement process involves a set of M+1 binary valued (1 or Ø) functions, defined on the image mesh, satisfying the following relation:

$$\sum_{\ell=0}^{m} \lambda_\ell(k) = 1 \qquad (2.2)$$

for any k=1,..., N^2. Relation (2.2) indicates that only one function λ_ℓ can be non-zero at any time k.

In the replacement process formulation of a picture, it is assumed that the image consists of a set of "objects" defined over the entire picture, each of these associated with a function λ_ℓ , and that the picture luminance values can be written as:

$$s(k) = \sum_{\ell=0}^{m} s_\ell(k)\, \lambda_\ell(k) \qquad (2.3)$$

$k=1,\ldots,N^2$, where s_ℓ represents the gray level values of the object 1.

It is worthwhile to note from this representation that: 1) at any pixel, only one object is present, i.e., there is no superposition of object luminances, 2) the functions λ_ℓ , being binary, carry the object boundary information without providing insight as to the pixel (local) properties of the objects themselves.

Of particular interest in the sequel is the case when M=1. Relation (2.2) becomes:

$$\lambda_0(k) + \lambda_1(k) = 1 \qquad (2.4a)$$

which is rewritten as

$$[\,1 - \lambda(k)\,] + \lambda(k) = 1\,. \qquad (2.4b)$$

Relation (2.4b) simply indicates that knowledge of either binary function (λ_0 , λ_1) is all that is needed. By convention, from here on, the binary function λ , referred to as

the replacement function, will characterize the object location. This implies the assignment of $(1-\lambda)$ to the so-called background (the object with luminance s_0).

Let us illustrate the replacement formulation by a few examples.[1] Fig. (2.1a) shows an image containing a square (object) of gray level value s_0 on a background of zero luminance. Along with it, also indicated, are the luminance of the object, the replacement function on three typical lines and the image brightness function. Fig. (2.1b) depicts the same set of functions indicated in Fig. (2.1a) as they apply to a picture containing two rectangles having the same constant intensity. However, because objects are defined by assumption on the whole image plane, their grey level functions are identical. Hence, only one replacement function is used. Even more, when the object appears repeatedly throughout the image, it is clear by the preceding method, that only one replacement function is necessary. The two schematic pictures appearing in Fig. (2.2) besides representing two more examples of the replacement process formulation, serve to introduce the concept of "horizontal convexity" as used in [29].

Horizontal Convexity : an object is said to be

(1) For clarity, the diagrams are drawn with continuous lines.

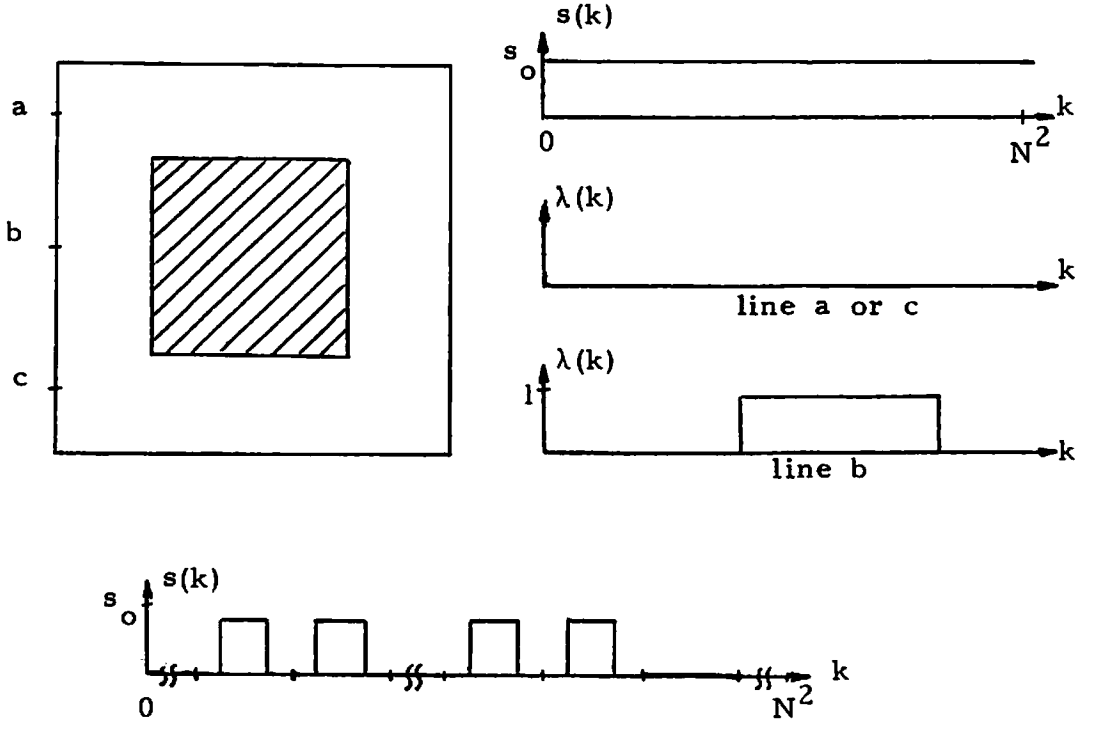

(a)

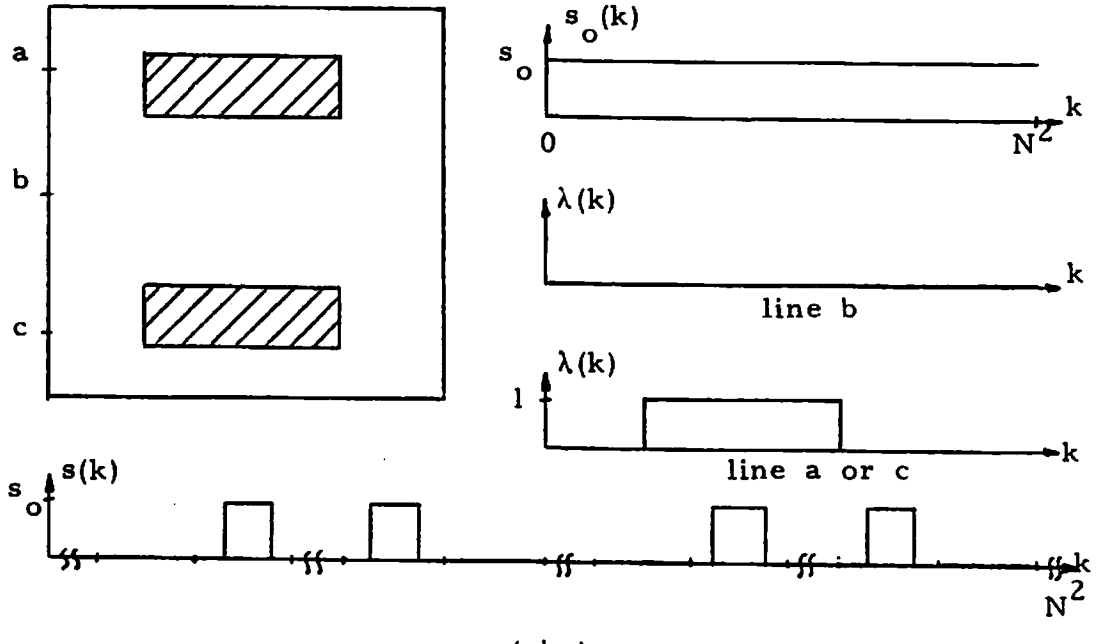

(b)

Fig. 2.1. Two images and their replacement models.

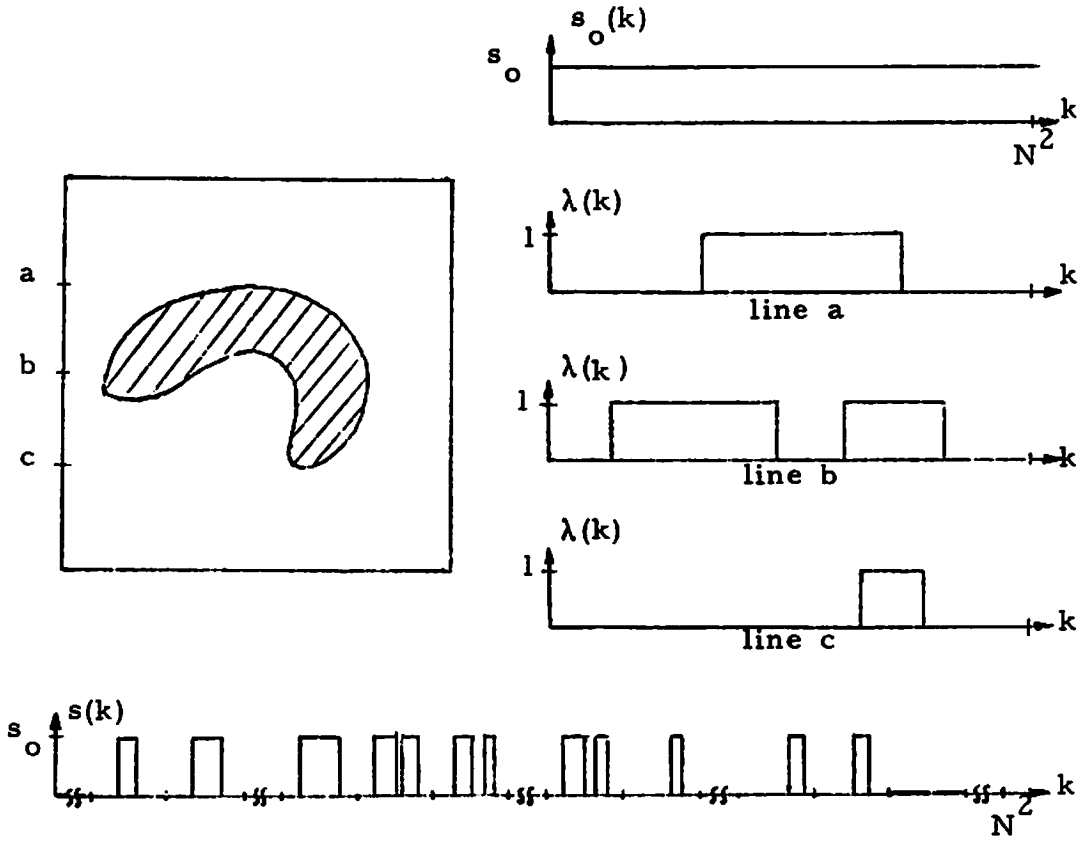

(a) Object not Horizontally Convex

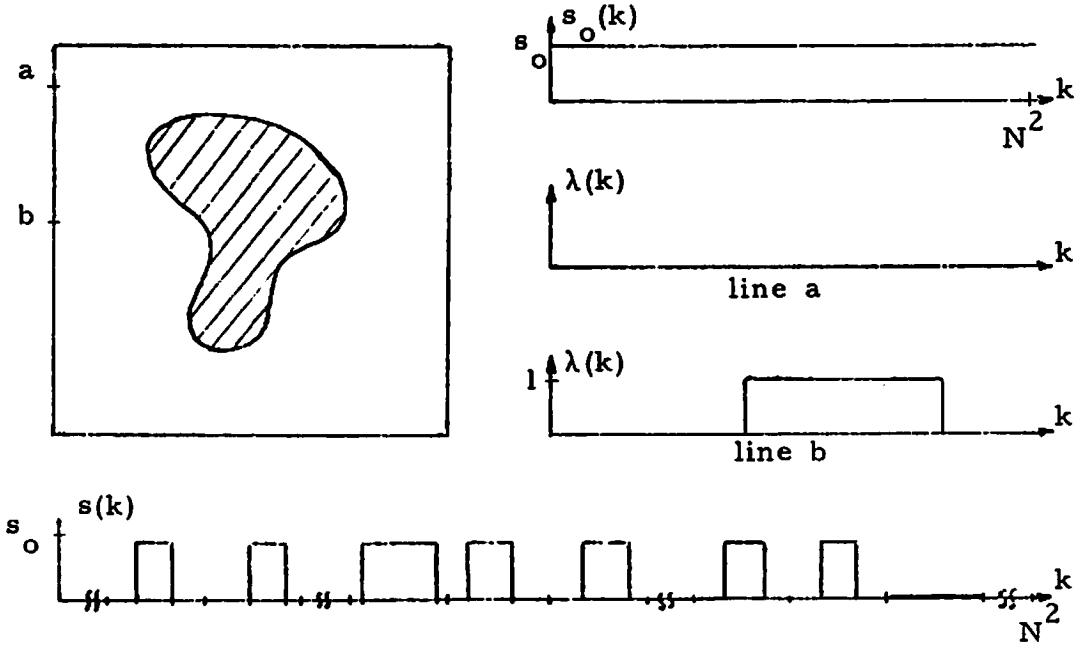

(b) Horizontally Convex Object

Fig. 2.2. Two images and their replacement models.

horizontally convex. if whenever two pixels, located on the same line, belong to the object, then any pixels between them also belong to the object.i.e.. let

$$\mathcal{O} = \{\text{object pixels}\}$$

if (j,m), $(j,n) \in \mathcal{O}$ and $m < n$, then $(j,m+1),\ldots,(j,n-1) \in \mathcal{O}$.

Examples of objects satisfying this property appear in Fig. (2.1) and Fig. (2.2b), while Fig. (2.2a) shows an object that is not horizontally convex as is evidenced from the plots of $\lambda(k)$ on line b and the image brightness function.

The purpose of this work is the development of recursive algorithms applicable to the determination of boundaries of horizontally convex objects from observations where the degradation phenomena are characterized by additive zero mean white Gaussian noise of variance σ^2 . viz,

$$y(k) = s(k) + v(k) \qquad (2.5)$$

$k=1,\ldots,N^2$. In images with brightness values given by

$$s(k) = \lambda(k)\, s_o(k) + [1 - \lambda(k)]\, s_b(k) \qquad (2.6)$$

$k=1,\ldots,N^2$. With s_o, s_b, representing the gray scale values of the object and background respectively, two statiscally independent cyclostationary random sequences whose first and second order statistics are known [21,34,35]. The statistics of the replacement function

(sequence) of λ in (2.6) are also known, but these will be specified later.

Note that due to the definition of λ , and in view of equation (2.6), the determination of the object boundary implies the determination of the replacement function and vice versa.

Let us consider more carefully the sequence of observations indicated in (2.5),(2.6). There will be some ones belonging to lines where $\lambda(k)$ is zero everywhere, i.e., the object being absent from those lines. On other lines, $\lambda(k)$ will be unity or zero on some pixels, depending on the observation origin, whether the object or the background. This consideration, then allows us to dichotomize the set of observations (2.5) as follows:

$$H_0 : y(k) = s_b(k) + v(k) \qquad k \in I_\phi$$

$$H_1 : y(k) = \lambda(k)\, s_o(k) + [1 - \lambda(k)]\, s_b(k) + v(k) \qquad k \notin I_\phi \qquad (2.7)$$

with $I = \{$lines where the object is absent$\}$.

From (2.7), it is clear that determination of the object boundary entails the selection of the lines where the object is present (detection of the object) and secondly, the boundary estimation per se. It is our objective here, to develop an optimal procedure to carry out the combined operations of detection and estimation of

object boundaries. Let us begin by introducing a representation for the binary function λ.

Representation of the Replacement Function λ

The binary function λ represents the existence ($\lambda(k)=1$) and absence ($\lambda(k)=\emptyset$) of object in the image at pixel k. Each k clearly corresponds, by the ordering rule, to a particular image line. Hence, it is possible to associate, on these lines where the object exists, to each k, two variables w(k) and c(k) representing the width and the geometrical center (measured from the midpoint on the picture) of the object at the associated line (see Fig. (2.3)). For instance, all k where $(j-1)N+1 \leq k \leq jN$, belong to the j-th line and to each corresponds the same width and center value, those of the j-th line. Thus

$$\begin{aligned} w(k+1) &= w(k) \qquad (j-1)N+1 \leq k \leq jN-1 \\ c(k+1) &= c(k) \qquad j \notin I_{\emptyset} \quad . \end{aligned} \tag{2.8}$$

The functions w(k) and c(k) are square wave functions taking on constant values over each line.

The replacement function $\lambda(k)$, $k=1,\ldots,N^2$, can now be defined in terms of w(k) and c(k) as follows:

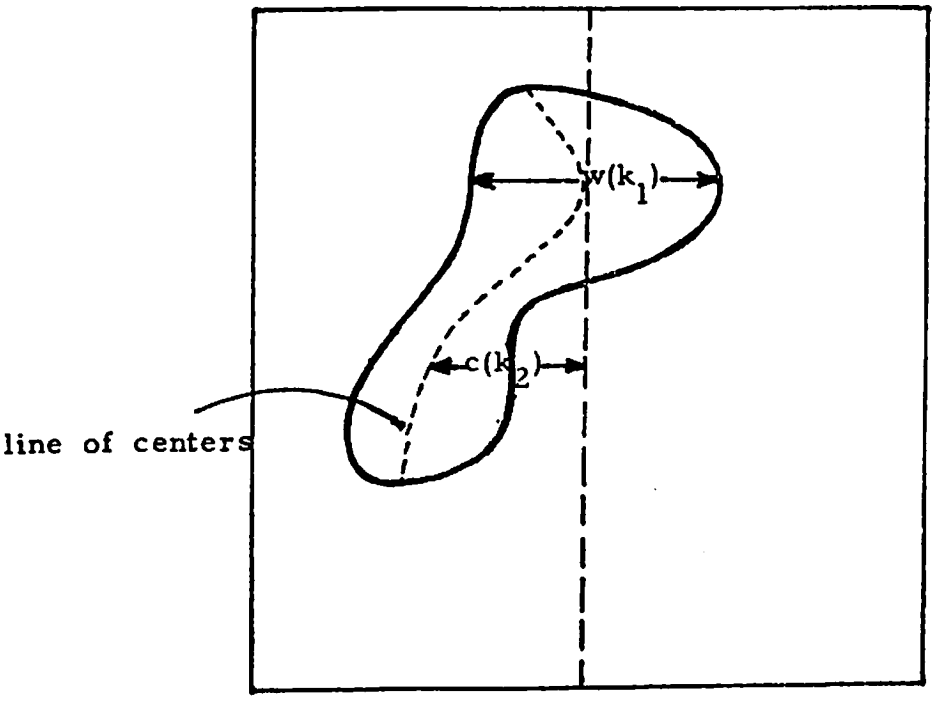

Fig. 2.3 Centers and widths at two different lines

$$\lambda(k) = \begin{cases} 0 & k \in I_{\phi} \\ 1 & (j-1)N + \frac{N}{2} + c(k) - \frac{w(k)}{2} \le k \le (j-1)N \\ & \quad + \frac{N}{2} + c(k) + \frac{w(k)}{2} \quad , \quad j \notin I_{\phi} \\ 0 & (j-1)N + 1 \le k < (j-1)N + \frac{N}{2} + c(k) - \frac{w(k)}{2} \quad , \quad j \notin I_{\phi} \\ 0 & (j-1)N + \frac{N}{2} + c(k) + \frac{w(k)}{2} < k \le jN \quad , \quad j \notin I_{\phi} \, . \end{cases} \qquad (2.9)$$

Since the object width is a positive quantity and the object must lie within the image, w(k) and c(k) satisfy the following constraints

$$w(k) \ge 0 \qquad (2.10a)$$

$$\frac{w(k)}{2} + |c(k)| \le \frac{N}{2} \, . \qquad (2.10b)$$

The quantities w(k) and c(k) are random sequences with known first and second order statistics. Let

$$w(k) = \tilde{w}(k) + \bar{w} \qquad (2.11a)$$

$$c(k) = \tilde{c}(k) + \bar{c} \qquad (2.11b)$$

where $\bar{w}$ and $\bar{c}$ are the mean values respectively. The quantity $\bar{w}$ is a rough measure of the size of the object while $\bar{c}$ is an indication of its probable (based on a priori

information) location within the picture. The latter quantity is likely to be zero in many applications. The zero mean random sequences $\tilde{w}(k)$ and $\tilde{c}(k)$ possess statistics which are measures of variation of object size and of object "skewness" over the ensemble of objects that the class of images to be processed comprises.

Let us digress for a moment so as to bring out the present development. From the replacement process formulation of images, it was observed that boundary estimation was accomplished by estimating the replacement functions (sequences) in the case of several objects or by estimation of the replacement function associated with the object when dealing with images composed of foreground and background. Being the replacement sequence binary, any estimation procedures resulting in non-binary estimates are unacceptable. After all, an estimate of $\lambda(k)$ equal to .3 across a picture is meaningless; what is needed is the location of the object if present, as indicated by unit estimates or its absence, corresponding to zero estimates. An alternative way to proceed, instead of estimating directly the replacement function is provided by the representation (2.9). The determination of λ can be reverted to the estimation of parameters with an intuitive geometric interpretation, which besides, are not restricted to be either zero or one. This digression is closed by indicating that to perform the recursive estimation of $w(k)$

and c(k), from the set of nonlinear observations (2.7), (2.9), it remains only to establish dynamic models representing the evolution of said parameters.[1]

Let us define the object vector r(k) by

$$r(k) \doteq [\, \tilde{w}(k) \quad \tilde{c}(k) \,]' \qquad (2.12)$$

where prime denotes transpose, and with abuse of notation $\tilde{w}(k)$ and $\tilde{c}(k)$ represent the real valued counterparts to $\tilde{w}(k)$ and $\tilde{c}(k)$ (w(k) and 2c(k) are integer valued).

As a first order approximation, the 2-dimensional vector r(k) is assumed to satisfy a first order Markov sequence,

$$r(k) = A_o(k)\, r(k) + B_o(k)\, u_o(k) \qquad (2.13)$$

where $u_0(k)=[u_1 \;\; u_2]'$ is a zero mean white normal sequence with unit covariance. Furthermore from (2.8), it follows that

$$A_o(k) = I \qquad \text{(the identity matrix)}$$

$$B_o(k) = 0$$

for all k except $k=jN$, $j \notin I_\phi$. For values of $k=jN$; $j, j+1 \in I_\phi$, (2.13) yields

(1) This assertion is correct if $s_o(k)$ and $s_b(k)$ are given or if from the second order statistics given, dynamic models for them have already been obtained.

$$r(jN+1) = A_o(jN)\, r(jN) + B_o(jN)\, u_o(jN)$$

but

$$r(jN+1) = r(jN+2) = \ldots = r[(j+1)N-1] = r[(j+1)N]$$

hence

$$r[(j+1)N] = A_o(jN)\, r(jN) + B_o(jN)\, u_o(jN) \qquad (2.14)$$

Note that $r(jN)$, for $j \notin I_\phi$ represents the width and center values associated with each of the object lines. Consequently, the matrices $A_o(jN)$ and $B_o(jN)$ determine the dependence of the object width and center on successive lines.

Let us comment upon the approximation mentioned just before (2.13). It is clear that instead of considering the evolution of $c(k)$, $w(k)$ as obtainable from the images, it was chosen to model the real valued parameters. It is understood that as much as digital images are a means of representation they result in certain restrictions not present on the natural scene or natural object, for instance, specifically, w and 2c are not restricted to be integers on the natural objects, although they so appear on a digital display. The problem of how to select the appropriate mesh for a digitized picture is not addressed here, rather, it is assumed that the avialable data possess adequate resolution for the objects of interest so that differences between the pictured derived parameters and

their real valued counterparts obtained from the natural objects are negligible.

The second type of approximation refers to the evolution model proposed here. The simplicity of the model (2.13) itself is intuitively appealing. Besides, it is in accordance with the often observed feature that object boundaries are generally smoothly varying. At any rate, depending on the available a priori information regarding the classes of objects investigated, this model represents exactly those a priori statistics or it may correspond to a lower order dynamic model approximation to the model derived from such statistics. Let us point out, that in a vast majority of occasions these a priori statistics are missing. Instead, sample images are available. In such instances it is first necessary to develop the appropriate statistics and consequently the model, or develop the model directly from the given samples [36].

CHAPTER THREE

The Optimal Structure

It has been indicated before that the object boundary determination, in addition to an estimation problem entails one of detection as well.

It is the purpose of this chapter to derive the necessary structure for boundary estimation and subsequently develop formulas for the optima estimator and detector that minimize a criterion to be given.

Many types of estimation-detection problems arise, ranging from pure detection where multiple hypotheses testing is required becoming intractable as the number of hypotheses increases, to cases where estimation and detection are performed at every pixel. For an example of the latter procedure, in the case of images modeled as 2-indexed fields, see [32,37,38]. The detection-estimation scheme that will be considered in the following has been motivated by the modeling of the class of images described before. To be more specific, the model considers pixel attributes like the luminance values of the object and background as well as line attributes indicated by the

object parameters (width, center). Inherent to the modeling of these last parameters is the necessity to test the object existence at each line.

It was Middleton and Esposito [39] who first formulated and solved, under a statistical decision theory framework, the simultaneous problems of detection and estimation. Since then, several authors [39-46] have considered applications that involve signal or parameter estimation under uncertainty. Common to all of these applications, however, is the assumption that the signals or parameters to be estimated are of "energy-type."

Let us explain the reason of the previous quotations with two simple examples. First, let us assume it is necessary to estimate the amplitude of the sinusoidal waves produced by a transmitter. Because of defective components in the receiver, this latter instrument observes the signal and noise (with known *a priori* probability) or noise alone. Second, suppose that in a meteorological station, where the probability of rain is known *a priori*, it is desired to estimate the temperature of the water drops from observations containing a signal (characteristic of the rain) and noise or noise alone. It is obvious that both these examples involve estimation under uncertainty. However, there is a difference between them: when the signal is not present, in the first case, the received

amplitude is zero and equivalently, for a zero amplitude emitted signal, the observation will contain noise only (there is no way the receiver could differentiate which one of these alternatives occurred). In the second instance, on the contrary, the reception of no signal is not indicative of hail, but represents the absence of rain. Hail itself corresponds to some signal. The amplitude is an example of an "energy-type" parameter (as used in [44]) in the sense that the absence of signal carries the implication of a zero parameter while the temperature is an instance of a "hypothesis dependent" parameter, meaningful only under a certain hypothesis.

The present formulation, as opposed to the cited applications, is concerned with the estimation of "hypothesis dependent" parameters.

Let us specify the tasks required to estimate the boundaries, and in so doing, define the necessary processor: at the end of every line, it is necessary to screen the observation data and produce a decision at the output, γ_o, indicating the absence of the object (when H_o is decided). When H_1 is decided (γ_1), proceed to estimate the width and center, and present these estimates at the output (see Fig. (3.1)), where γ_i is the decision associated with hypothesis H_i. In other words, the boundary processor output must be either a decision or an

estimate.

In order to quantify the actions carried out by the two components illustrated in Fig. (3.1) costs will be associated to the detection as well as the estimation stage. It is natural to ask at this point: what are the estimator and detector (decision rule) that minimize the average cost of joint detection and estimation over the ensemble of possible observations ?

To the answer of this question, along the lines of [39], the rest of this section is devoted, but first it is necessary to introduce some notation. Let us define:

p_i , $i=0,1$: the <u>a priori</u> probability of occurrence of hypothesis H_i.

$Y(j)=\{y(k),y(k-1),\ldots,y(k-N+1) : k=jN,\ j=1,\ldots,N\}$

$r_{est}(jN|Y(j))$[1] : an estimate of the object boundary $r(jN)$ at the j-th line, given the observation $Y(j)$.

$\delta(\gamma_i|Y)$[2] : the decision rule that assigns 0 or 1 to each decision γ_i , depending on the observation Y.

$c_{i,\ell}$, $i,\ell=0,1$: the detection cost incurred when

(1) In the following, for simplicity, the arguments of $Y(j)$, $r_{est}(jN|Y(j))$, $r(jN)$, $\delta(\gamma_i|Y(j))$ will be eliminated, unless required for clarity of the context.
(2) This means that $\delta(\gamma_i|Y)$ is a non-randomized decision. The results that follow do not make use of this condition, and they would have been valid, if instead, randomized decisions would have been allowed.

deciding γ_i when actually H_ℓ occurred.

$f_{1,0}$: the cost of estimating a boundary when no object is present.

$f_{1,1}(r_{est}, r)$: the cost of estimating the object boundary $r(jN)$ by $r_{est}(jN|Y(j))$, when an object is present (H_1 is true) and γ_1, has been decided.

$p(Y|r, H_1)$ [1] : the probability density of $Y(j)$ given $r(jN)$ and when H_1 is true.

Let us comment on the rationale for the preceding costs, before proceeding any further. First of all, it is clear that the global cost of estimation and detection must reflect the various ways in which correct or wrong decisions as well as different estimate values affect the overall performance of the processor. On the other hand, the set of costs needs to be defined in the context of the application and effects of the processor implementation.

Six different costs have been introduced, four directly associated with the detector and the other two directly associated with the estimator. These 6 costs can be considered as element costs in the sense that they apply whenever the detector produces a decision or the estimator presents an estimate. As schematized in Fig. (3.1)

(1) Similar definitions apply for $p(Y|H_0)$ and $p(r|H_1)$.

though, the processor outputs are generally the result of a decision and an estimation. consequently any input-output relation for the processor will involve one or more of these basic costs. Thus, in this latter respect. the aforementioned six costs can be grouped in four global processor costs representing the costs associated with processing observation data and resulting in an output. be it a decision or an estimate. Namely,

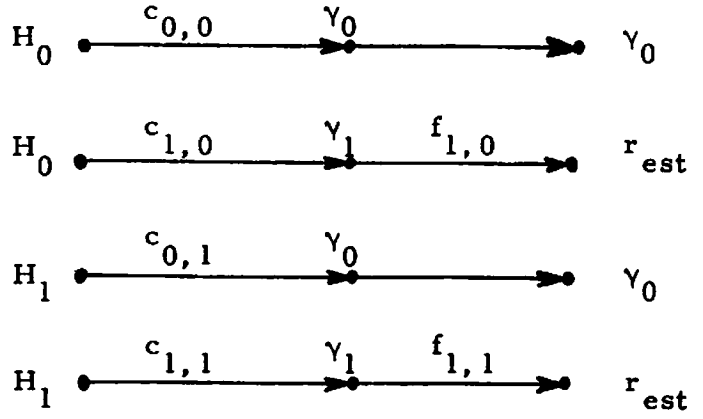

In this representation. the hypothesis shown on the left, states the observation origin, while the output is specified on the extreme right. In between, the intermediate steps and accompanying costs are indicated.

The four element costs $c_{i,\ell}$ were chosen as constants, in agreement with the classical procedure that assigns a constant cost to every decision whether it is misclassification or correct classification. More importantly though, such selection discriminates (weighs) the data as follows: when the observation data belong to a

line where the background is present and the detector makes the correct decision, then $c_{0,0}$ represents a fixed charge in using the detector. When the data belong to a line where the object is present, if the detector produces a wrong decision (misses the object) then, the detector incurs a penalty $c_{0,1}$. Note that this penalty is imposed regardless of the object (of the object parameters) involved. Note also, that the previous charges ($c_{0,1}$ or $c_{0,0}$) are the only costs the processor will incur, for any observations resulting in the output decision γ_0. Similar remarks apply to $c_{1,0}$ and $c_{1,1}$. However, as in both these cases the processor operations are not restricted to the detector but include the activation of the estimator as well, the effect on the data is better appreciated in combination with the estimation charges.

As a starter, the pair $c_{1,0}, f_{1,0}$ is applied in those instances where the data are wrongly classified resulting in estimates of nonexistent objects. The cost $c_{1,0}$ penalizes any such decisions stemming from the detector. Penalties for the estimate are not clear. This is so, because all estimated parameters are undesirable, in fact, they are meaningless. A constant estimation cost ($f_{1,0}$), however, assumes the absence of any "preferred" estimates and it is therefore chosen. Finally, there is the selection of $f_{1,1}$. As the object is present and an estimate is produced, the fidelity of reproduction

criterion should mandate the form of this cost function. In general though, it is a function of both the object parameters and their estimates and as such it has been indicated by $f_{1,1}(r_{est}, r)$.

Recall that it is necessary to determine the average cost of joint detection and estimation R_{D+E}. With the previous definitions, it follows that:

$$
\begin{aligned}
R_{D+E} = \int dY \{ & \delta(\gamma_0|Y)[p_0\, c_{0,0}\, p(Y|H_0) \\
& + p_1\, c_{0,1} < p(Y|r,H_1) > r] \\
& + \delta(\gamma_1|Y)[p_0\, c_{1,0}\, p(Y|H_0) \\
& + p_1\, c_{1,1} < p(Y|r,H_1) > r] \\
& + \delta(\gamma_1|Y)[p_0\, f_{1,0}\, p(Y|H_0) \\
& + p_1 < f_{1,1}(r_{est}, r)\, p(Y|H_1) > r]\} \qquad (3.1a) \\
= \int dY \{ & \delta(\gamma_0|Y)[p_0\, c_{0,0}\, p(Y|H_0)] \\
& + \delta(\gamma_0|Y)[p_1\, c_{0,1} < p(Y|r,H_1) > r] \\
& + \delta(\gamma_1|Y)\, p_0[c_{1,0} + f_{1,0}]\, p(Y|H_0) \\
& + \delta(\gamma_1|Y)\, p_1 < [c_{1,1} + f_{1,1}(r_{est}, r)] \\
& p(Y|r,H_1) > r\} \qquad (3.1b)
\end{aligned}
$$

where

$$< p(Y|r,H_1) > r \doteq \int p(Y|r,H_1)\, p(r|H_1)\, dr = p(Y|H_1)\,.$$

The three terms on the right hand side (RHS) of (3.1a) represent the costs associated with deciding the absence of the object, deciding its presence and estimating the object boundary, this grouping being based on the estimator or detector related actions. On (3.1b) however, the costs are grouped with an input-output perspective in mind; they represent the global costs associated with producing an estimate (2 costs), and with outputting decision γ_0 (the first two terms on the RHS). Assuming the set of costs in (3.1) to be positive, it can be seen that minimization of R_{D+E} (with respect to δ and r_{est}) is equivalent to minimizing the integrand $R_{d+e}(\delta, r_{est})$,

$$
\begin{aligned}
R_{d+e}(\delta^*, r^*) &= \min_{\delta, r_{est}} R_{d+e}(\delta, r_{est}) \\
&= \min_{\delta, r_{est}} \{\delta(\gamma_0|Y)[p_0\, c_{0,0}\, p(Y|H_0) \\
&\quad + p_1\, c_{0,1}\, p(Y|H_1)] \\
&\quad + \delta(\gamma_1|Y)[p_0(c_{1,0} + f_{1,0})\, p(Y|H_0) \\
&\quad + p_1 < [c_{1,1} + f_{1,1}(r_{est}, r)]\, p(Y|r, H_1) > r]\} \\
&= \min_{\delta} \{\delta(\gamma_0|Y)[p_0\, c_{0,0}\, p(Y|H_0) \\
&\quad + p_1\, c_{0,1}\, p(Y|H_1)] \\
&\quad + \delta(\gamma_1|Y)[p_0(c_{1,0} + f_{1,0})\, p(Y|H_0) \\
&\quad + \min_{r_{est}} \{p_1 < [c_{1,1} + f_{1,1}(r_{est}, r)] \\
&\quad\quad p(Y|r, H_1) > r\}]\} .
\end{aligned}
\qquad (3.2)
$$

From (3.2) it can be seen that the minimization can be done in two steps. First with respect to r_{est} for any decision rule, and second with r_{est} replaced by the optimal estimate, the optimal decision rule can be derived. The defining relations for the optimal estimator and detector are consequently:

$$< f_{1,1}(r^*, r)\, p(Y|r, H_1) > r = \min_{r_{est}} < f_{1,1}(r_{est}, r)\, p(Y|r, H_1) > r \,. \tag{3.3}$$

Decide the object is present ($\delta^*(\gamma_1|Y)=1$, $\delta^*(\gamma_0|Y)=\emptyset$) when:

$$p_0(c_{1,0} + f_{1,0})\, p(Y|H_0) + \{p_1 < [c_{1,1} + f_{1,1}(r^*, r)]\, p(Y|r, H_1) > r\}$$
$$\leq p_0\, c_{0,0}\, p(Y|H_0) + p_1\, c_{0,1}\, p(Y|H_1) \,. \tag{3.4}$$

Otherwise, decide the object is absent ($\delta^*(\gamma_0|Y)=1$, $\delta^*(\gamma_1|Y=\emptyset)$.

A special case of interest, in the sequel, is obtained when the cost of estimation is chosen to be the quadratic error.

Quadratic Error Cost :

$$f_{1,1}[r_{est}(jN|Y(j), r(jN)] = (r_{est} - r)'(r_{est} - r) \,. \tag{3.5}$$

The procedure indicated by (3.3) becomes,

$$
\begin{aligned}
&< f_{1,1}(r^*, r)\, p(Y|r, H_1) > r \\
&= \min_{r_{est}} < (r_{est} - r)'(r_{est} - r)\, p(Y|r, H_1) > r \\
&= \min_{r_{est}} \int (r_{est} - r)'(r_{est} - r)\, p(Y|r, H_1)\, p(r|H_1)\, dr \\
&= \min_{r_{est}} \int (r_{est} - r)'(r_{est} - r)\, p(r|Y, H_1)\, p(Y|H_1)\, dr \\
&= p(Y|H_1) \min_{r_{est}} \int (r_{est} - r)'(r_{est} - r)\, p(r|Y, H_1)\, dr . \qquad (3.6)
\end{aligned}
$$

In view of the last equality, it is well known that r^* minimizing (3.6) corresponds, in this case, to:

$$r^*[jN|Y(j)] = E[r(jN)|Y(j), H_1] . \qquad (3.7)$$

Letting,

$$P^*[jN|Y(j), H_1] = P^* = \int (r^* - r)(r^* - r)'\, p(r|Y, H_1)\, dr \qquad (3.8)$$

and replacing (3.7), (3.8) into (3.4),

$$
\begin{aligned}
&p_0(c_{1,0} + f_{1,0})\, p(Y|H_0) + p_1(c_{1,1} + tr\, P^*)\, p(Y|H_1) \\
&\leq p_0\, c_{0,0}\, p(Y|H_0) + p_1\, c_{0,1}\, p(Y|H_1) . \qquad (3.9)
\end{aligned}
$$

Where tr indicates trace, in general, the detection costs satisfy:

$$c_{1,0} - c_{0,0} > 0$$

$$c_{0,1} - c_{1,1} > 0 \qquad (3.10)$$

which penalize more heavily wrong decisions. Collecting terms in (3.9) and using (3.10), it follows that (see(3.4))

$$p_1(c_{0,1} - c_{1,1} - \text{tr } P^*)\, p(Y|H_1) \geq p_0(c_{1,0} + f_{1,0} - c_{0,0})\, p(Y|H_0) \geq 0. \qquad (3.11)$$

Therefore, the optimal detector decisioning becomes:

$$\left.\begin{aligned} \delta^*(\gamma_1|Y) &= 1 \\ \delta^*(\gamma_0|Y) &= 0 \end{aligned}\right\} \quad \text{if} \quad \left\{\begin{aligned} &K_c > 0 && (3.12a) \\ &\text{and} \\ &\Lambda_{j,jN} \geq K^* && (3.12b) \end{aligned}\right.$$

$$\left.\begin{aligned} \delta^*(\gamma_0|Y) &= 1 \\ \delta^*(\gamma_1|Y) &= 0 \end{aligned}\right\} \quad \text{if} \quad \left\{\begin{aligned} &K_c \leq 0 && (3.13a) \\ &\text{or} \\ &K_c > 0 && (3.13b) \\ &\text{and} \\ &\Lambda_{j,jN} < K^* && (3.13c) \end{aligned}\right.$$

where,

$$K_c = c_{0,1} - c_{1,1} - \text{tr } P^*$$

$$K^* = (c_{1,0} + f_{1,0} - c_{0,0})/K_c$$

$$\Lambda_{j,jN} = \frac{p_1\, p[Y(j)|H_1]}{p_0\, p[Y(j)|H_0]} \quad , \quad j = 1,\ldots,N \qquad (3.14)$$

Fig. (3.2) corresponds to the quadratic error boundary processor indicated in (3.7), (3.12), (3.13), where the interdependence between the detection and the estimation stages has been shown explicitly. Note that the switch, (in Fig. (3.1)) operated by the detector has been delayed with respect to the estimator.

Two more cost functions and their associated optima processors are considered in Appendix A. The first processor while useful for estimating hypothesis-dependent parameters (HDP) involves a detector with different costs for non-detection. In particular, the penalty incurred when missing big objects is greater that the one charged for small objects. Although the resulting estimator is identical to (3.7), the detector threshold now depends on the parameter estimate and covariance instead of the covariance only. Energy-type parameter (ETP) estimation is provided by the second processor. A clear difference of this processor from the previous ones is that it always produces an estimate at its output; furthermore, the estimator found no longer performs estimation under certainty of observation but besides, involves the evaluation of a fraction with values between zero and one. The detector threshold is a function of the estimate obtained without uncertainty.

It is important to compare the cost functions resulting in (3.7),(3.12), (3.13) with the costs (A.8) in order to understand the basic differences involved in estimating these two parameter classes. Note that in ETP estimation each decision has an associated estimate; in this particular case (case 2 of appendix A), when γ_0 is decided, said value is zero, while r_{est} is associated with γ_1. On the contrary, no estimate can properly be associated to decision γ_0 in HDP estimation. Note also that with ETPs, the set of parameters under H_0 corresponds to $\{r=\emptyset\}$, but that no such representation exists for HDPs. These idiosyncrasies are manifested on the second and third costs; these are the costs incurred when deciding erroneously. The estimation penalty on the second line in (A.8) depends on r_{est}^2. However, as the true value of the parameter is $r=\emptyset$, this penalty indeed is a function of the squared of the estimation error. For the HDP case, the estimation cost is independent of the estimate provided; this serves to penalize the <u>action</u> of false alarming regardless of any geometric considerations of the estimated object. In fact, as there is no object (H_0), any estimate is equally undesirable. The third estimation cost in (A.8) penalizes as a function of r^2. However, as the output estimate is zero, such cost then depends on the squared of the estimation error. In HDP estimation, the cost $c_{0,1}$ is constant. Such a cost is necessary to ensure that <u>any</u>

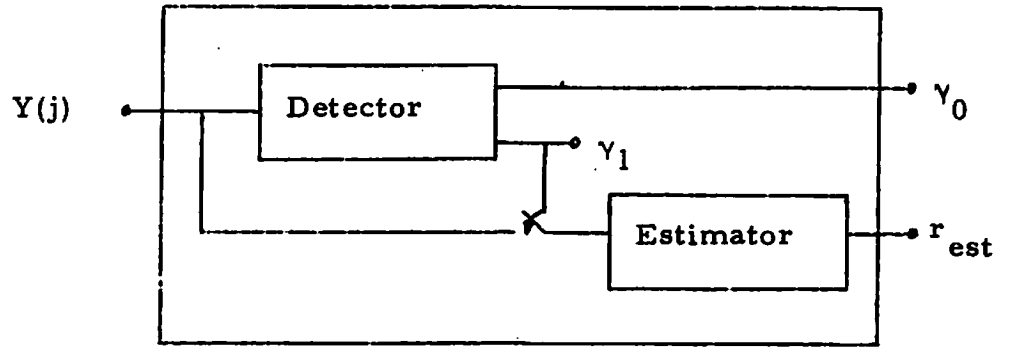

Fig. 3.1. Boundary processor.

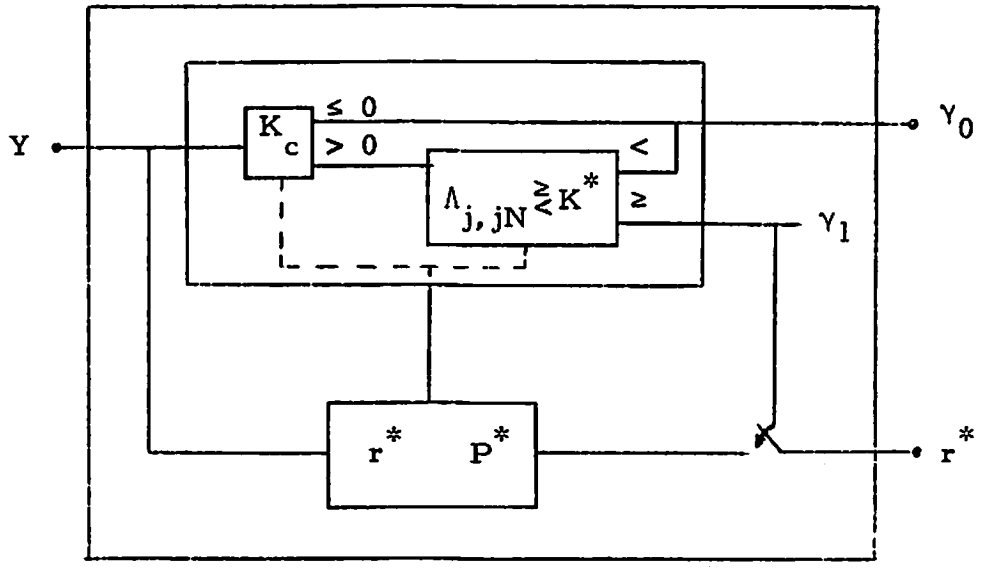

Fig. 3.2. Quadratic error boundary processor.

any object missed is penalized identically.

It must be pointed out, upon reflection on the costs used, that the joint estimation-detection considered before has been treated in isolation from other lines. In fact, more general situations involving the joint scheme could be obtained by a set of costs that not only weighs the results of decisions in the present line but of future ones as well.

It is necessary to turn our attention to the implementation of (3.7) as well as (3.14). Although the optimum detector is defined in terms of (3.12), (3.13), it is clear that the successful evaluation of the likelihood ratio (3.14) is of paramount importance to be able to use the former two relations. The next two sections will be dedicated to the implementation of the components appearing in Fig. (3.2).

The Estimator

This section is concerned with the choice of a general estimation procedure having desirable computational properties while being applicable to the problem at hand. Let the n-dimensional vector x(k) be defined by

$$x(k) = [\, r(k)' \quad z(k)' \,] \tag{3.15}$$

where r(k) is the object vector $[\tilde{w}(k) \ \tilde{c}(k)]'$ and z(k) represents the random processes associated with the object and background textural information, $s_o(k)$ and $s_b(k)$. The latter quantities can, in general, be modeled by first order Markov processes [29,31,32]. This along with (2.13) results in a linear model for x(k),

$$x(k) = A(k)\, x(k) + B(k)\, u(k) \qquad (3.16)$$

with u(k) being a zero mean white normal sequence with identity covariance matrix. The observation given by (2.7) is highly nonlinear due to the structure of (2.7) and the binary nature of $\lambda(k)$ given by (2.9).

From the computational point of view, considering that the amount of data is generally very large (a typical image is decomposed into $(256)^2$ pixels or more) it is desired that: (a) the estimator be of recursive nature and (b) the information transferred to any step of recursion from the previous step be of limited nature (e.g., first and second order moments only). The latter requirement is important because recursivity alone does not necessarily reduce the computational burden. In fact, a very general recursive procedure for determination of the a posteriori probability density is available [33], albeit completely impractical. The extended Kalman filter and its variations are a set of filters that meet both these requirements [34-36]. However, these estimators require linearization of the

system, including the observation equation, at each recursion step. This is not possible here due to the type of nonlinearity involved, in particular, the binary nature of $\lambda(k)$ as expressed by (2.9).

To be more specific, let us define the estimate of $x(k-1)$ and its covariance at time k-1 (i.e., after $y(k-1)$ has been received) by $\hat{x}(k-1|k-1)$ and $P(k-1|k-1)$ respectively.

Considering a restriction on information transfer, first and second order statistics only, the information available to obtain the estimate of $x(k)$ at time k is $\hat{x}(k-1|k-1)$, $P(k-1|k-1)$ and $y(k)$. From (3.16), this leads to a predicted estimate and a covariance of $x(k)$ (before $y(k)$ is received):

$$\begin{aligned}\hat{x}(k|k-1) &= E[x(k)|\hat{x}(k-1|k-1),\ P(k-1|k-1),\ y(k-1)] \\ &= A(k-1)\,E[x(k-1)|\hat{x}(k-1|k-1),\ P(k-1|k-1),\ y(k-1)] \\ &\quad + B(k-1)\,E[u(k-1)|\hat{x}(k-1|k-1),\ P(k-1|k-1),\ y(k-1)] \\ &= A(k-1)\,\hat{x}(k-1|k-1). \qquad (3.17)\end{aligned}$$

Similarly,

$$\begin{aligned}P(k|k-1) &= E\{[x(k)-\hat{x}(k|k-1)][x(k)-\hat{x}(k|k-1)]'|\hat{x}(k-1|k-1), \\ &\qquad P(k-1|k-1),\ y(k-1)]\} \\ &= A(k-1)\,E\{[x(k-1)-\hat{x}(k-1|k-1)][x(k-1)-\hat{x}(k-1|k-1)]'| \\ &\qquad \hat{x}(k-1|k-1),\ P(k-1|k-1),\ y(k-1)]\}\,A'(k-1)\end{aligned}$$

$$+ B(k-1)\,B'(k-1)$$

$$= A(k-1)\,P(k-1|k-1)\,A'(k-1) + B(k-1)\,B'(k-1). \quad (3.18)$$

Equations (3.17) and (3.18) express $\hat{x}(k|k-1)$ and $P(k|k-1)$ in terms of $\hat{x}(k-1|k-1)$ and $P(k-1|k-1)$.

Consequently, the MMS estimate of $x(k)$ and its covariance given the above information are given by

$$X_{MMS}(k|k) = E[x(k)|\hat{x}(k|k-1),\ P(k|k-1),\ y(k)] \quad (3.19)$$

$$P_{MMS}(k|k) = E[x(k) - X_{MMS}(k|k)][x(k) - X_{MMS}(k|k)]'|\hat{x}(k|k-1),$$

$$P(k|k-1),\ y(k)]\ . \quad (3.20)$$

By direct application of Bayes rule,

$$p[x(k)|\hat{x}(k|k-1),\ P(k|k-1),\ y(k)]$$

$$= \frac{p[x(k),\ y(k)|\hat{x}(k|k-1),\ P(k|k-1)]}{\int p[x(k),\ y(k)|\hat{x}(k|k-1),\ P(k|k-1)]\,dx(k)}\ . \quad (3.21)$$

Since $v(k)$ is an independent white noise,

$$p[x(k),\ y(k)|\hat{x}(k|k-1),\ P(k|k-1)]$$

$$= p[y(k)|x(k)]\ p[x(k)|\hat{x}(k|k-1),\ P(k|k-1)]\ . \quad (3.22)$$

The probability density function $p[x(k)|\hat{x}(k|k-1),\ P(k|k-1)]$ appearing in (3.22) represents the knowledge on $x(k)$ <u>a priori</u> to the reception of $y(k)$. Determination of the exact form of this probability density is very

complicated and, in fact, requires transfer of information beyond the first and second order moments. Consequently, a density function will be "assigned" to this and denoted by $p_a[x(k)]$ satisfying the two given moments exactly. The assignment of this function, in light of computational considerations, is an approximation resulting in the estimate $\hat{x}(k|k)$ and its covariance $P(k|k)$ (this approximation is in lieu of the linearization in the extended Kalman filter, which is not applicable here). Explicit relations for $\hat{x}(k|k)$ and $P(k|k)$ are thus obtained by making the indicated change in (3.22),(3.21) and further replacing into (3.19) and (3.20),

$$\hat{x}(k|k) = \frac{\int x(k)\, p[y(k)|x(k)]\, p_a[x(k)]\, dx(k)}{\int p[y(k)|x(k)]\, p_a[x(k)]\, dx(k)} \qquad (3.23)$$

$$P(k|k) = \frac{\int [x(k) - \hat{x}(k|k)][x(k) - \hat{x}(k|k)]'\, p[y(k)|x(k)]\, p_a[x(k)]\, dx(k)}{\int p[y(k)|x(k)]\, p_a[x(k)]\, dx(k)} . \qquad (3.24)$$

Equations (3.23) and (3.24) along with (3.17) and (3.18) constitute the desired recursive estimator. The specific choice for $p_a(.)$, as well as its effect on the computational burden and performance of the estimator will be postponed until chapter four where two special cases of boundary estimation will be considered.

The Detector

An algorithm applicable to the evaluation of the likelihood ratio is determined in this section. Recall, the likelihood ratio (LR) was defined in (3.14) as:

$$\Lambda_{j,jN} = \frac{p_1\, p[Y(j)|H_1]}{p_0\, p[Y(j)|H_0]} \qquad j = 1,\ldots,N$$

$$= \frac{p_1\, p[y(jN),\ y(jN-1),\ \ldots,\ y((j-1)N+1|H_1]}{p_0\, p[y(jN),\ y(jN-1),\ \ldots,\ y((j-1)N+1|H_0]} \cdot \qquad (3.25)$$

The direct evaluation of (3.25) is a formidable task, in most cases, due to the dimensionality of the densities involved, and furthermore by the fact that each observation $y(k)$, $k=(j-1)N+1,\ldots, jN$ is random not only because of the additive noise $v(k)$, but also because the signal $s(k)$ is random as well.

However, for a related problem, dealing with the detection of a known signal $s(k)$ in white Gaussian noise, the evaluation of the LR is particularly simple [37]. It involves a "correlator" of the observation $y(k)$ with the signal $s(k)$, i.e., it requires the computation of $\sum y(k)s(k)$. Moreover, when detecting Gaussian signals $s(k)$ in additive white Gaussian noise [38], the evaluation of the LR also involves a "correlator," in this case, connecting the MMS estimate of the signal and the

observation y(k). The MMS estimator plays a recurrent role under more general conditions of detection as is evidenced in [39-41]. Kailath's [39] expressions for the LR in terms of the casual MMS estimator, and vice versa, unfortunately are defined in the Ito Calculus sense, and are applicable to continuous time problems. In the discrete case, even though relations resembling the ones for the continuous case exist (that express the LR as a function of the casual MMS estimator, and vice versa), their applicability is very restricted [42-46]. In summary, the difficulties associated with the direct evaluation of the LR have been pointed out. Furthermore, the close relation, in the context of detection, between MMS estimation and the LR has been indicated.

It is possible however, to view the LR in terms of a recursive expression. Let us define, in general for any k, $\Lambda_{j,k}$ by:

$$\Lambda_{j,k} = \frac{p_1\, p[y(k),\ y(k-1),\ \ldots,\ y((j-1)N+1)\,|\,H_1]}{p_0\, p[y(k),\ y(k-1),\ \ldots,\ y((j-1)N+1)\,|\,H_0]} \qquad (3.26)$$

$$j = 1,\ldots,N \quad , \quad (j-1)\,N+1 \le k \le jN \ .$$

Having defined $\Lambda_{j,k}$ as above, using the definition of conditional density, the fact that the additive noise v(k) is white, by application of Bayes rule and similarly to the procedure leading to (3.21), (3.22), it follows that

$$\Lambda_{j,k} = \{\{ \int p[y(k)|x(k)\ ,\ H_1]\ p[x(k)|y(k-1),\ldots,H_1]\ dx(k)$$

$$\Big/ \int p[y(k)|z(k)\ ,\ H_0]\ p[z(k)|y(k-1),\ldots,H_0]\ dz(k)\}$$

$$[\Lambda_{j,k-1}]\} \qquad (3.27a)$$

$$\Lambda_{j,(j-1)N} = p_1 / p_0 \qquad (3.27b)$$

where the density $p[y(k)|z(k),H_0]$ has been explicitly expressed in terms of $z(k)$ and not $x(k)$ because under the hypothesis H_0, the object boundary is undefined.

Finally, taking logarithms in (3.27a)

$$\ln \Lambda_{j,k} = \ln \{ \int p[y(k)|x(k)\ ,\ H_1]\ p[x(k)|y(k-1),\ldots,H_1]\ dx(k)$$

$$\Big/ \int p[y(k)|z(k)\ ,\ H_0]\ p[z(k)|y(k-1),\ldots,H_0]\ dz(k)\}$$

$$+ \ln \Lambda_{j,k-1} \qquad (3.28)$$

$$j = 1,\ldots,N \quad , \quad (j-1)N+1 \le k \le jN\ .$$

Comparison of (3.26) and (3.25) indicates that the LR is equal to $\Lambda_{j,k}$ at $k=jN$. Also, as (3.28) has been derived from (3.26), the former relation represents a recursive alternative to (3.25) in the evaluation of the LR.

The probability density $p[x(k)|\ y(k-1),\ldots,\ H_1]$ in (3.28) plays a central role in the MMS estimation of $x(k)$ given the past observations $y(k-1),\ldots,\ H_1$, because it

agglutinates the knowledge on x(k) a priori to the reception of y(k), and also because the first two moments of the density correspond to the MMS estimate and error covariance. However, it was indicated in the previous section, that as a result of constraints imposed on the estimation algorithm the available (forwarded) information on x(k) prior to the reception of y(k) consisted of $\hat{x}(k|k-1)$ and $P(k|k-1)$. Besides, the exact evaluation of $p[x(k)|\, y(k-1),\ldots,H_1]$, in most cases, was discarded as impractical. It is therefore necessary to resort to an approximation of the a priori density function (for an application when the approximating density is gaussian, see [47]). In the following, the conditioning variables in the prior density are replaced by the available statistics, and subsequently the procedure indicated in the estimator section is applied. The result is a recursive expression for $L_{j,k}$, an approximation to $\Lambda_{j,k}$,

$$\ln L_{j,k} = \ln \left\{ \int p[y(k)|x(k)\,,\, H_1]\, p_a[x(k)|H_1]\, dx(k) \right.$$
$$\left. \Big/ \int p[y(k)|z(k)\,,\, H_0]\, p_a[z(k)|H_0]\, dz(k) \right\}$$
$$+ \ln L_{j,k-1} \qquad (3.29a)$$

$$j = 1,\ldots,N \quad , \quad (j-1)N+1 \le k \le jN$$

$$L_{j,(j-1)N} = p_1 / p_0 \,. \qquad (3.29b)$$

It is convenient to point out regarding the evaluation of the likelihood ratio by the algorithm (3.29a), that the denominator in (3.23) and the numerator expression in (3.29a) are identical. The explicit appearance of H_1 in the latter one serves to stress the hypothesis, a datum that was unnecessary in the context of the preceding section. In later applications this fact is used to reduce the amount of computations required to evaluate the LR.

CHAPTER FOUR

Boundary Estimation for Binary Pictures

Binary images are those where the object and background luminance levels are constants, i.e.,

$$s_o(k) = s_o \quad ; \quad s_b(k) = s_b \ .$$

Two cases are considered here: one where s_o and s_b are known (hence only w(k) and c(k) remain to be estimated), the other when s_o and s_b are also unknown.

For the case of known luminances (x(k)=r(k)),

$$p[y(k)|x(k)] = \begin{cases} \dfrac{1}{2\pi\sigma^2} \exp - \dfrac{[y(k) - s_o]^2}{2\sigma^2} & \text{for } \lambda(k) = 1 \\ \dfrac{1}{2\pi\sigma^2} \exp - \dfrac{[y(k) - s_b]^2}{2\sigma^2} & \text{for } \lambda(k) = 0 \end{cases} \qquad (4.1)$$

where it is necessary to determine regions of the w and c plane where $\lambda(k)$ is zero or unity. These areas are illustrated in Fig. (4.1) and result from (2.10). Hence (3.23) and (3.24) become

$$\hat{x}(k|k) = \{ e^{-[y(k) - s_o]^2/2\sigma^2} \int_{\lambda=1}^{\infty} x(k)\, p_a[x(k)]\, dx(k)$$

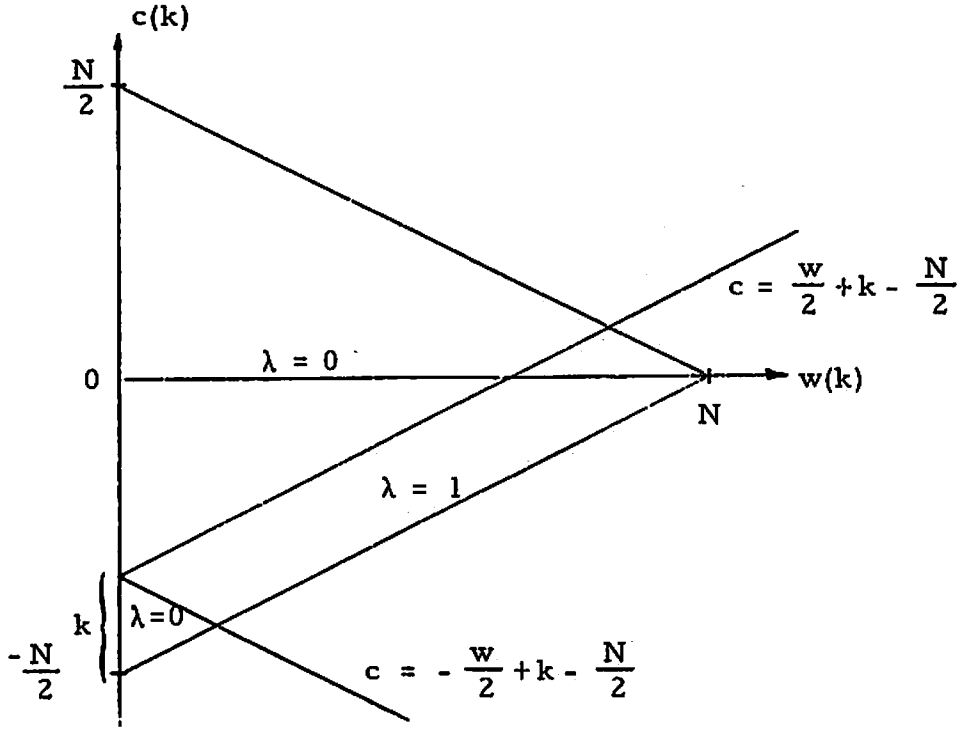

Fig. 4.1. $\lambda(k) = 1$ and $\lambda(k) = 0$ regions.

$$+ \; e^{-[y(k) - s_b]^2/2\sigma^2} \int_{\lambda=0} x(k)\, p_a[x(k)\, dx(k)\}$$

$$/ \; \{e^{-[y(k) - s_o]^2/2\sigma^2} \int_{\lambda=1} p_a[x(k)]\, dx(k)$$

$$+ \; e^{-[y(k) - s_b]^2/2\sigma^2} \int_{\lambda=0} p_a[x(k)]\, dx(k)\} \qquad (4.2)$$

$$P(k|k) = \{e^{-[y(k) - s_o]^2/2\sigma^2} \int_{\lambda=1} \{[x(k) - \hat{x}(k|k)][x(k) - \hat{x}(k|k)]'$$

$$p_a[x(k)]\, dx(k)\} + e^{-[y(k) - s_b]^2/2\sigma^2} \int_{\lambda=0} \{[x(k) - \hat{x}(k|k)]$$

$$[x(k) - \hat{x}(k|k)]'\, p_a[x(k)]\, dx(k)\}\}$$

$$/ \; \{e^{-[y(k) - s_o]^2/2\sigma^2} \int_{\lambda=1} p_a[x(k)]\, dx(k)$$

$$+ \; e^{-[y(k) - s_b]^2/2\sigma^2} \int_{\lambda=0} p_a[x(k)]\, dx(k)\}\,. \qquad (4.3)$$

When the background luminance is assumed known, the denominator in (3.29a) reduces to:

$$\int p[y(k)|z(k)\,,\, H_0]\, p_a[z(k)|H_0]\, dz(k) = \frac{1}{2\pi\sigma^2} \exp - \frac{[y(k) - s_b]^2}{2\sigma^2}\,. \qquad (4.4)$$

Consequently, the detector relationship to be evaluated becomes:

$$\ln L_{j,k} = \ln L_{j,k-1} + \frac{[y(k) - s_b]^2}{2\sigma^2}$$

$$+ \ln \{ e^{-[y(k) - s_o]^2/2\sigma^2} \int_{\lambda=1} p_a[x(k)]\, dx(k)$$

$$+ e^{-[y(k) - s_b]^2/2\sigma^2} \int_{\lambda=0} p_a[x(k)]\, dx(k) \} . \quad (4.5)$$

Let us now consider the case of unknown luminances, and further, assume that the probability density $p_a[x(k)]$ can be represented by:

$$p_a[x(k)] = p_a[r(k)]\, p_a[z_o(k)]\, p_a[z_b(k)] \quad (4.6)$$

where $z_o(k)$ and $z_b(k)$ correspond to the states, in the model (3.16), associated with the representation of the object and the background textures. For instance, if s_o and s_b are <u>a priori</u> (assumed) values for both textures, then z_o, z_b represent the deviation from such values and they are sought during the estimation, in other words:

$$z_o(k) = s_o - \bar{s}_o$$

$$z_b(k) = s_b - \bar{s}_b . \quad (4.7)$$

In order to simplify the expressions for $\hat{x}(k|k)$ and $P(k|k)$, let us first consider the denominator on (3.23), (3.24):[1]

(1)For readibility, the argument (k) has been dropped except in the last relation.

$$
\begin{aligned}
\text{DEN} &= \iiint p(y|x)\, p_a(r)\, p_a(z_o)\, p_a(z_b)\, dr\, dz_o\, dz_b \\
&= \iint \{ \int_{\lambda=1} p(y|x)\, p_a(r)\, p_a(z_o)\, p_a(z_b) \\
&+ \int_{\lambda=0} p(y|x)\, p_a(r)\, p_a(z_o)\, p_a(z_b) \}\, dr\, dz_o\, dz_b \\
&= \iint \{ p_a(z_b)\, p_a(z_o) \int_{\lambda=1} p(y|x)\, p_a(r) \\
&+ p_a(z_o)\, p_a(z_b) \int_{\lambda=0} p(y|x)\, p_a(r) \}\, dr\, dz_o\, dz_b \\
&= \iint \{ p_a(z_b)\, p_a(z_o)\, p(y|z_o) \int_{\lambda=1} p_a(r) \\
&+ p_a(z_o)\, p_a(z_b)\, p(y|z_b) \int_{\lambda=0} p_a(r) \}\, dr\, dz_o\, dz_b \\
&= \{ [\int p_a[z_b(k)]\, dz_b(k)] [\int p[y(k)|z_o(k)]\, p_a[z_o(k)]\, dz_o(k)] \\
&\quad [\int_{\lambda(k)=1} p_a[r(k)]\, dr(k)] \} + \{ \int p_a[z_o(k)\, dz_o(k)] \\
&\quad [\int p[y(k)|z_b(k)]\, p_a[z_b(k)]\, dz_b(k)] [\int_{\lambda(k)=0} p_a[r(k)]\, dr(k)] \}
\end{aligned}
\qquad (4.8)
$$

where $p[y(k)|z_o(k)]$ and $p[y(k)|z_b(k)]$ show the explicit dependence of $p[y(k)\ x(k)]$ in the regions where the object or the background is present, i.e., these densities represent the counterpart to (4.1) for the case of unknown luminance.

The calculation of (3.23) by the same procedure used to obtain (4.8) results in:

$$
\begin{aligned}
(\hat{r}' \hat{z}_o' \hat{z}_b')'(k|k) = \{\{[\int (0' \; 0' \; z_b')' \, p_a[z_b(k)]\, dz_b(k)] \\
[\int (0' \; z_o' \; 0')' \, p[y(k)|z_o(k)]\, p_a[z_o(k)]\, dz_o(k)] \\
[\int_{\lambda(k)=1} (r' \; 0' \; 0')' \, p_a[r(k)]\, dr(k)]\} \\
+ \{[\int (0' \; z_o' \; 0')' \, p_a[z_o(k)]\, dz_o(k)] \\
[\int (0' \; 0' \; z_b')' \, p[y(k)|z_b(k)]\, p_a[z_b(k)]\, dz_b(k)] \\
[\int_{\lambda(k)=0} (r' \; 0' \; 0')' \, p_a[r(k)]\, dr(k)]\}\} / DEN \; .
\end{aligned}
$$

(4.9)

In a similar fashion (3.24) can be evaluated. For simplicity, only the term $[\hat{r}(k)-r(k|k)]\,[\hat{r}(k)-r(k|k)]'$ is presented in the following. Other terms like $[z_i(k)-\hat{z}_i(k|k)][z_i(k)-\hat{z}_i(k|k)]'$, i=o,b can be obtained by replacing the former expression on the left hand side by the latter ones and performing the appropriate groupings on the RHS:

$$
\int \{[r(k) - \hat{r}(k|k)][r(k) - \hat{r}(k|k)]' \, p[y(k)|x(k)]\, p_a[x(k)]\}\, dx(k) / DEN
$$

$$
= \{\{[\int p_a[z_b(k)]\, dz_b(k)][\int p[y(k)|z_o(k)]\, p_a[z_o(k)]\, dz_o(k)]
$$

$$\left[\int_{\lambda(k)=1} [r(k) - \hat{r}(k|k)][r(k) - \hat{r}(k|k)]' \, p_a[r(k)\, dr(k)]\right]$$

$$+ \{[\int p_a[z_o(k)]\, dz_o(k)][\int p[y(k)|z_b(k)]\, p_a[z_b(k)]\, dz_b(k)]$$

$$\left[\int_{\lambda(k)=0} [r(k) - \hat{r}(k|k)][r(k) - \hat{r}(k|k)]' \, p_a[r(k)]\, dr(k)]\right]\} / DEN\,. \qquad (4.10)$$

It is important to comment, at this point, on the preceding set of relations. First of all in (4.2), (4.3) the final evaluation is ultimately dependent on the probability density $p_a[x(k)]=p_a[r(k)]$ and furthermore, on how the two integrations are performed. Secondly, the particular form (4.6) is necessary to arrive at the simple relations (4.8)-(4.10), where $p_a[r(k)]$ or more specifically the integrations over the $\lambda=0$ and $\lambda=1$ regions present the same characteristics cited above.

The detector relation (3.29a) becomes, in this case:

$$\begin{aligned} \ln L_{j,k} &= \ln L_{j,k-1} - \ln\{\int p[y(k)|z_b(k)\,,\, H_0]\, p_a[z_b(k)|H_0]\, dz_b(k)\} \\ &\quad + \ln DEN \\ &= \ln L_{j,k-1} - \ln\{\int p[y(k)|z_b(k)]\, p_a[z_b(k)]\, dz_b(k) \\ &\quad + \ln DEN\,. \end{aligned} \qquad (4.11)$$

Note that in order to perform detection by the procedure outlined, it is only necessary to accumulate two by-products of the estimation stage, avoiding this way any

need for any new calculations.

Next, we return to the choice of the probability density function $p_a[x(k)]$ such that its first two moments be equal to $\hat{x}(k|k-1)$ and $P(k|k-1)$ respectively. From an information point of view [15], for a given mean and variance, the normal distribution represents the maximum uncertainty (entropy); consequently a Gaussian density would be a conservative choice. However, this directly violates the precise a priori knowledge that the random variables $w(k)$ and $c(k)$ as well as $z_o(k)$ and $z_b(k)$ are bounded in magnitude (the first ones represent the center and width of the object on a given image while the latter ones are the luminance values of the texture, constrained by the imaging system). A choice that satisfies this requirement and completely avoids the necessity of any numerical integrations, is to select independent uniform densities for $w(k)$ and $c(k)$ (and z_o, z_b for the case of unknown luminance). Fig. (4.2) shows a typical region of integration when uniform densities are used.

It was stated above that as a result of the choice of a uniform density for $p_a[x(k)]$, no integrations were necessary. This fact in view of the comments on equations (4.2)-(4.10) was one of the attributes sought from the approximating density.

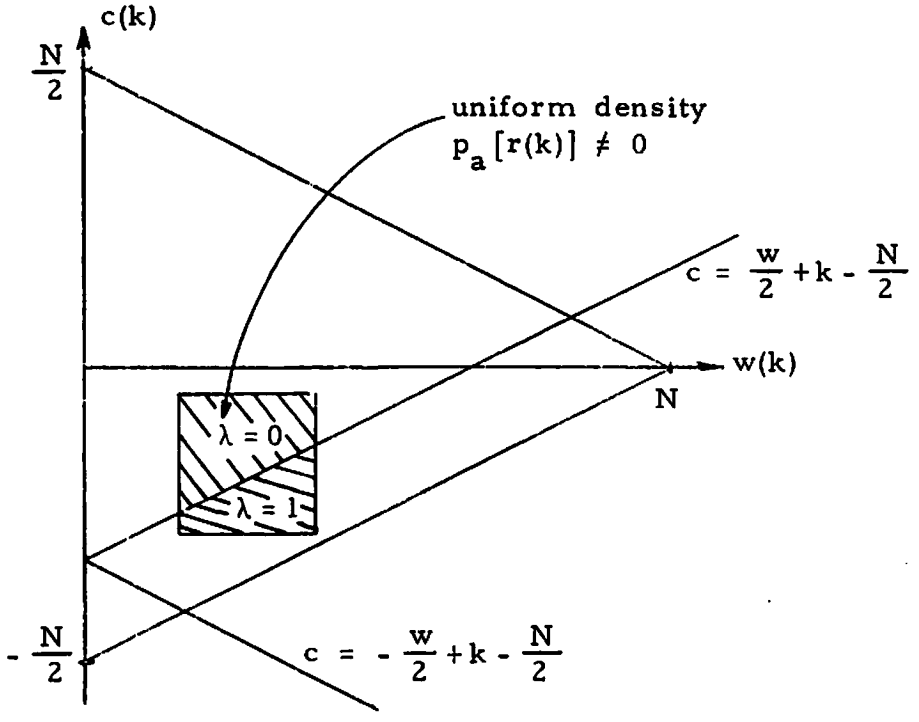

Fig. 4.2. $\lambda(k) = 0$ and $\lambda(k) = 1$ regions with uniform density.

Let us consider in the following, the steps necessary to carry out the above integrations. Although Fig. (4.2) represents a typical case (to be explained later), without much thought one can see that there is no reason to believe the region where $p_a[r(k)]$ is different from zero should lie completely inside the triangular area defined by (2.10) in the w, c plane (albeit $\hat{r}(k|k-1)$ does). In fact, Fig. (4.3) presents an enumeration of the possible interceptions. Two possible alternatives result from the last figure: first, it is possible to disregard (2.10) entirely and proceed to integrate over the corresponding original rectangular region (where $p_a[r(k)] \neq 0$). Second, the validity of the density function can be restricted to the interception, but then a new density has to be found. In this dissertation the second alternative has been taken, where the new density has been assumed uniform and different from zero in the intercepting region of the w, c plane. It must be pointed out that an error is likely to be introduced by either alternative, except, in the case shown in Fig. (4.2) where both approaches coincide and no error is generated. When (2.10) is not accounted for, this error refers to contributions to the integrals from w,c pairs in $\square$ (symbol definition below) but outside Δ. When the density is modified to account for (2.10), the error refers to the difference in moments of the modified and original density defining $\square$.

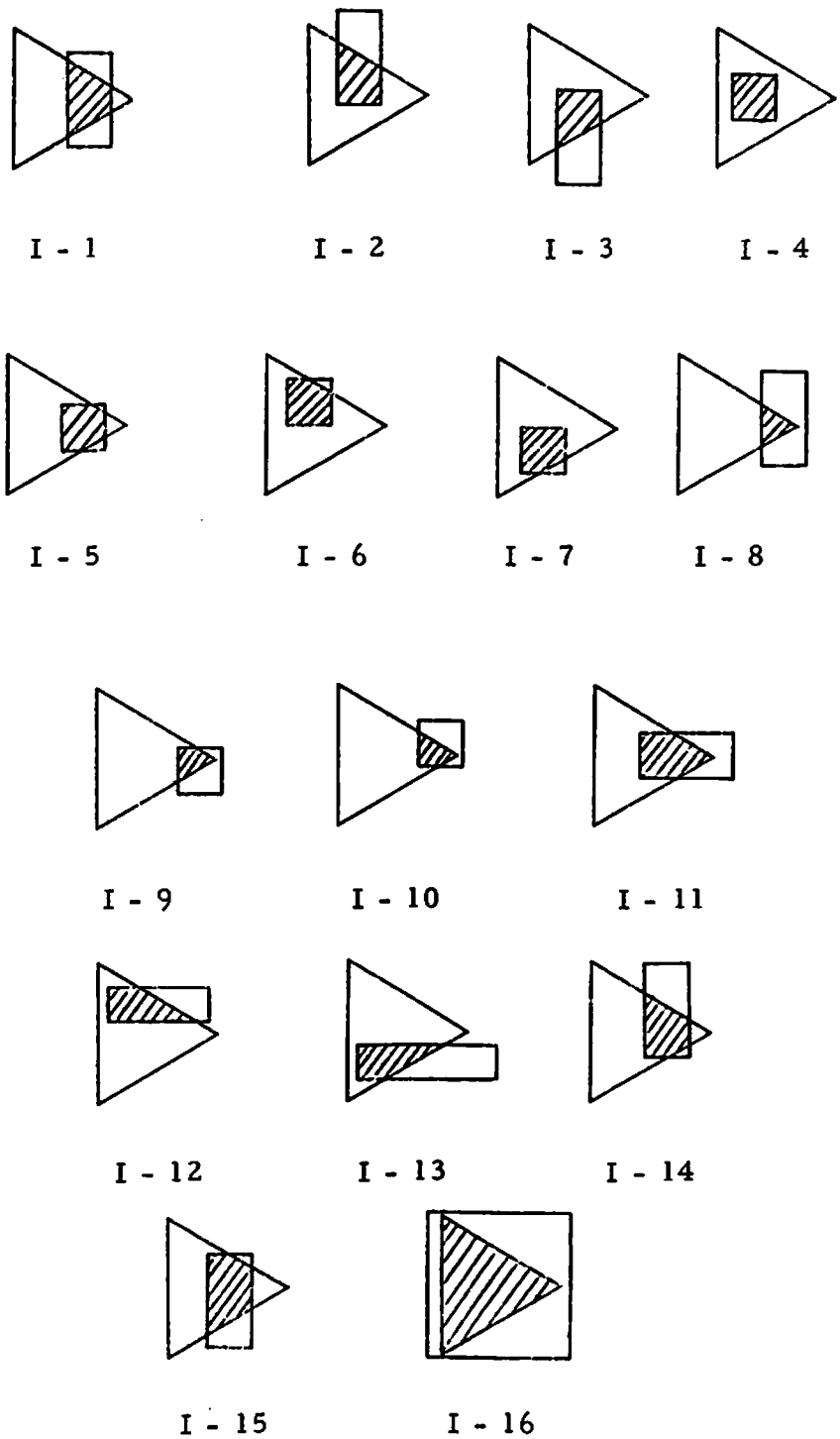

Fig. 4.3. Possible interceptions (hatched areas) of uniform density $p_a[r(k)] \neq 0$ with region defined by (2.10).

In other words, if $\cap$ denotes interception, and if:

$$\square = \{(w(k)\ ,\ c(k)\ :\ p_a[r(k)] \neq 0\}$$

$$\Delta = \{(w(k)\ ,\ c(k)\ :\ w(k) \geq 0\ ,\ \frac{w(k)}{2} + \frac{|c(k)|}{2} \leq \frac{N}{2}\ \}$$

then, it is necessary to perform the following integrations (see (4.2.), (4.3), (4.8)-(4.10)):

$$\begin{array}{ll} \int_{(\lambda=0)\cap(\square\cap\Delta)} dr(k) & \int_{(\lambda=1)\cap(\square\cap\Delta)} dr(k) \\ \int_{(\lambda=0)\cap(\square\cap\Delta)} r(k)\, dr(k) & \int_{(\lambda=1)\cap(\square\cap\Delta)} r(k)\, dr(k) \\ \int_{(\lambda=0)\cap(\square\cap\Delta)} r'(k)\, r(k)\, dr(k) & \int_{(\lambda=1)\cap(\square\cap\Delta)} r'(k)\, r(k)\, dr(k)\ . \end{array} \qquad (4.12)$$

Because of the variety of shapes the regions $(\lambda=\emptyset)\cap(\square\cap\Delta)$ and $(\lambda=1)\cap(\square\cap\Delta)$ can take, the integrations (4.12) have been carried out analytically on the set shown in Fig. (4.4). Each region in (4.12) can be viewed as a mosaic of the latter simpler polygonal areas (see Fig. (4.5) for an example). This in turn, reduces the integration to a search for a mosaic and a simple numerical evaluation.

Although there are 16 different interceptions drawn in

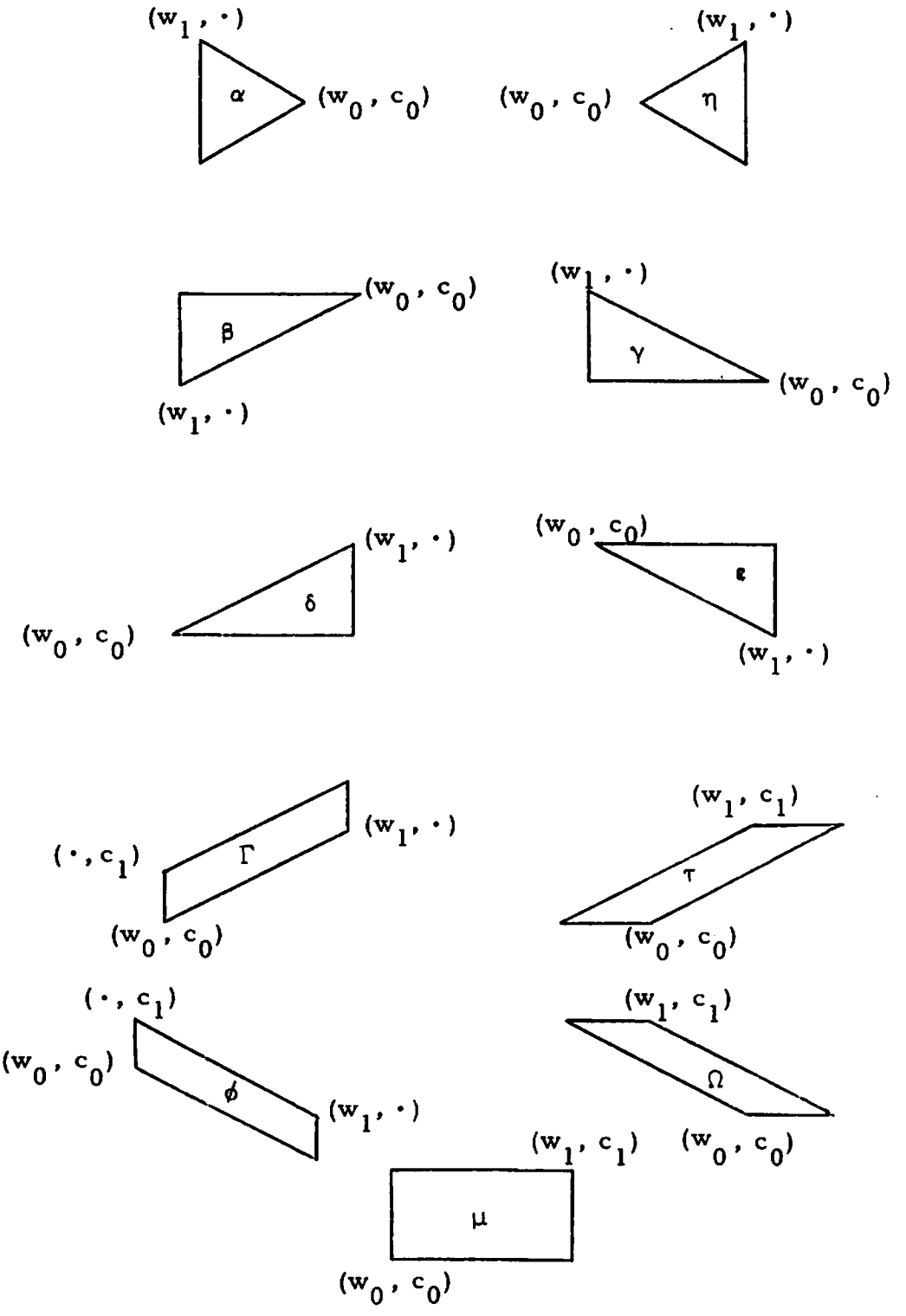

Fig. 4.4. Polygonal areas where integrations (4.12) are calculated. Shown are the parameters that define each polygon.

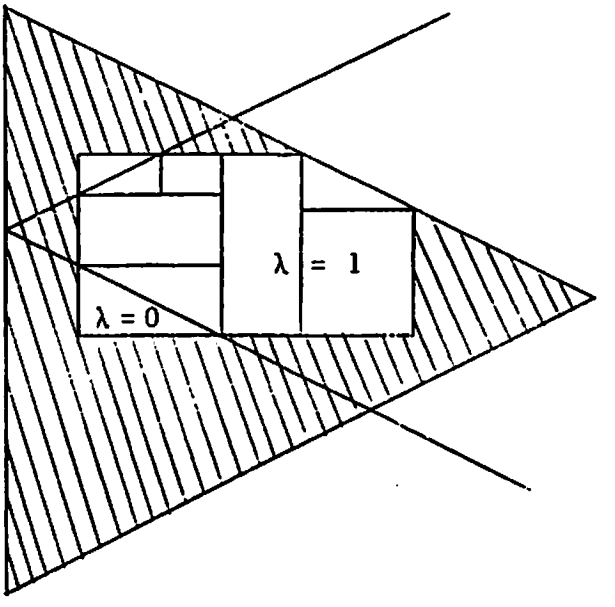

Fig. 4.5. Example of a (□∩Δ) region mosaic.

Fig. (4.3), experimental results indicate that frequently only four cases (I-4,I-5,I-6,I-7) occur, with the case depicted in Fig. (4.2) being the most frequent.

Experimental Procedures

The purpose of the foregoing chapters has been the motivation on the subject of boundary estimation, the derivation of an optimal boundary processor minimizing the average costs of joint detection-estimation in noisy imagery and the subsequent recursive implementation of a suboptimal processor, based on first and second order moments.

This section deals with the application of the boundary processor to a set of images and the presentation of these results as visual evidence to its capabilities.

In chapter two, it was shown that the replacement function was expressible in terms of geometric characteristics of the objects, these geometric properties being the width and center. In consequence, modeling the binary function implied testing as to the foreground presence plus a model for the geometry itself. In the modeling of the geometric characteristics, the continuous counterparts of the width and center were assumed expressed

in terms of a first order Markov sequence. Hence, to be able to apply the processor relations, the first step necessarily must be the determination of the matrices appearing in (3.16), which in turn are defined by the class of objects under investigation.

In the following the boundary processor will be applied to a set of 256X256 binary images containing an ellipse. An elliptical form has been chosen because by changing five parameters, different orientation, location and size objects can be readily obtained. Besides, ellipses are examples of horizontally convex objects.

To illustrate the procedure followed in determining the matrices in (2.14), let us assume for simplicity that only one ellipse of fixed orientation, size and position needs to be estimated. This assumption seems quite restrictive because in general more than one ellipse may need to be detected. Later on it will be dropped. Nevertheless, the procedure could be considered as a way "to tune" the processor. Let us further assume that,

$$\tilde{w}[(j+1)N] = a_w \tilde{w}[jN] + b_w u_w(jN) \qquad (4.13)$$

i.e., the Markov model is stationary and decoupled (another relation similar to (4.13) governs $\tilde{c}$). The former supposition greatly reduces the number of parameters to be determined while at the same time allows varying degrees of

boundary smoothness or ruggedness to be accomodated through the choice of a_w, b_w. Decoupling is a resonable assumption that otherwise would be indicative of geometrical dependences within the image between widths and object locations.

But from (4.13),

$$E\{\tilde{w}[(j+1)N]\,\tilde{w}(jN)\} = a_w\, E\{\tilde{w}^2(jN)\} + b_w\, E\{\tilde{w}(jN)\, u_w(jN)\}$$

$$= a_w\, E\{\tilde{w}^2(jN)\} \qquad (4.14)$$

similarly,

$$E\{\tilde{w}[(j+\ell)N]\,\tilde{w}(jN)\} = a_w^{\ell}\, E\{\tilde{w}^2(jN)\} \qquad (4.15)$$

also from (4.13) and (4.14),

$$E\{\tilde{w}^2[(j+1)N]\} = a_w\, E\{\tilde{w}[(j+1)N]\,\tilde{w}(jN)\}$$

$$+ b_w\, E\{\tilde{w}[(j+1)N]\, u_w(jN)\}$$

$$= a_w^2\, E\{\tilde{w}^2(jN)\} + b_w^2 \qquad (4.16)$$

therefore,

$$E\{\tilde{w}^2(jN)\}[1 - a_w^2] = b_w^2 \qquad (4.17)$$

Determination of a_w commences with equation (4.15). In the absence of ensemble averages, sample statistics have been used instead. Further, a_w has been chosen to minimize a function of the sample averages. More explicitly, if the

object is J lines "long," Σ and Σ' correspond to $\Sigma_{j=1}^{J}$ and $\Sigma_{j=1}^{J-\ell}$ respectively, then(1)

$$\begin{aligned}
&\Sigma' [w(j+\ell) - \bar{w}_s][w(j) - \bar{w}_s] \\
&= \Sigma' w(j+\ell)\, w(j) + (J-\ell)\, \bar{w}_s^2 - \bar{w}_s \Sigma' [w(j+\ell) + w(j)] \\
&= a_{w_s}^{\ell} (J-\ell)\, V_s^2 \qquad (4.18)
\end{aligned}$$

where

$$\bar{w}_s = \Sigma\, w(j) / J$$

$$V_s^2 = \Sigma\, [w(j) - \bar{w}_s]^2 / J\,,$$

(4.18) can be considered the defining relation for $a_{w_s}^{\ell}$. Thus

$$\begin{aligned}
a_{w_s}^{\ell} = \{ &\Sigma' w(j+\ell)\, w(j) + (J-\ell)\, \bar{w}_s^2 \\
&- \bar{w}_s [-w(1) - \ldots - w(\ell) - w(J) - \ldots - w(J-\ell+1) + 2J\, \bar{w}_s]\} \\
&/ (J-\ell)\, V_s^2 \,. \qquad (4.19)
\end{aligned}$$

The expression on the RHS of (4.19) is a function of l, g(l). Now, a_w has been chosen to be the value of a that minimizes for known n and L

$$\sum_{\ell=1}^{L} [\ln g(\ell) - \ell \ln a]^2 / \ell^n \,. \qquad (4.20)$$

(1) For simplicity, the index has been shortened to j, e.g., w(j)=w(jN).

Carrying out the minimization ($a \neq 0$), it follows that

$$a_w = \exp\{ \sum_{\ell=1}^{L} \ell^{(1-n)} \ln g(\ell) / [\sum_{\ell=1}^{L} \ell^{(2-n)}]] . \qquad (4.21)$$

In particular, for $n=0$,

$$a_w = \exp\{6 \sum_{\ell=1}^{L} \ell \ln g(\ell) / [L(L+1)(2L+1)]\} . \qquad (4.22)$$

Equation (4.22) for $L=10$ has been used to determine a_w. b_w follows from (4.17) through use of the sample variance V_s^2,

$$b_w^2 = (1 - a_w^2) V_s^2 . \qquad (4.23)$$

Values of a_w in (4.21) for $n=1,2$ were very close to the ones obtained from (4.22) and were not considered further.

The previous method and comments apply to the center parameters as well, when the application involves several objects or more than one object size, orientation or location, by the procedure detailed before a set of parameters has been obtained, which in turn has been averaged to produce the final parameter values.

To generate the observations, the original set of pictures, containing an ellipse with random location, orientation and size and unit luminance on a background of zero luminance, was corrupted by additive white Gaussian

noise of variance σ^2. Figs. (4.6a,b), (4.7a,b) illustrate some of the observations. Luminance values exceeding one have been displayed as 1 and those below zero as Ø.

Two different boundary processors have been implemented.

Case 1: To single out the boundary estimation <u>per se</u>, the processor was provided with the luminance values of the object and background. Hence, a 2-state estimator (x(k)=r(k)) was used.

Several detection costs were utilized throughout the experiments and they have been appended to the resulting pictures as three numbers separated by commas. They represent, from left to right: (1) if this number (call it K) is different from Ø, a constant threshold, $K^*=K$, has been used. In this case, the two numbers on the right are meaningless. This constant value in contrast to a threshold dependent on the covariance of the estimate has been used at low noise levels because both produce identical results. When K=Ø, a variable threshold has been used as the numbers on the right indicate. (2) This number is equivalent to $c_{0,1}-c_{1,1}$. (3) This is $c_{1,0}+f_{1,0}-c_{0,0}$. Succinctly:

$$\begin{aligned} &1.\quad K^* \\ &2.\quad c_{0,1} - c_{1,1} \\ &3.\quad c_{1,0} + f_{1,0} - c_{0,0} \end{aligned} \qquad (4.24)$$

The parameters used on this processor were:

$$N = 256 \quad \bar{w} = 57. \quad \bar{c} = 0. \quad p_0 = .5 \quad p_1 = .5 \qquad (4.25)$$

with matrices $A_o(jN)=A_o$ and $B_o(jN)=B_o$ given by:

$$A_o = \begin{pmatrix} .926 & 0 \\ 0 & .97 \end{pmatrix} \qquad B_o = \begin{pmatrix} 7.78 & 0 \\ 0 & 2.91 \end{pmatrix} .$$

In (4.25) the sample statistics were used on w,c, while the a priori probability of object presence or absence was assumed equally likely. The initial conditions

$$\hat{r}(0|0) = \begin{pmatrix} 0 \\ 0 \end{pmatrix} \qquad P(0|0) = \begin{pmatrix} 20^2 & 0 \\ 0 & 50^2 \end{pmatrix}$$

indicate the uncertainty on the intial estimates prior to the reception of the observations. When the processor output was γ_o, the estimator was reinitialized to these same values before processing a new line of observations.

Results from applications of said processor are illustrated in Figs. (4.6c), (4.7c) and (4.7d) where for clarity, the estimated boundary (dimmer trace) has been superposed on the original ellipse (brighter trace). When coincidence of the estimate and the original has occurred,

the trace has been left dim.

Case 2: In this occasion the object luminance is constant as in the previous case, although unknown. The processor (estimator) has been supplied with a priori statistics about $s_o(k)$ in the form of the average and variance.

$$E\,S_o = .5 \qquad E(S_o - E\,S_o)^2 = E\,\tilde{S}_o^2 = .05\,.$$

Relations (4.24), (4.25) remain applicable as before, however the matrices A(jN)=A and B(jN)=B now correspond to

$$A = \begin{pmatrix} .926 & 0 & 0 \\ 0 & .97 & 0 \\ 0 & 0 & 1 \end{pmatrix} \qquad B = \begin{pmatrix} 7.78 & 0 & 0 \\ 0 & 2.91 & 0 \\ 0 & 0 & 0 \end{pmatrix}$$

with initial conditions given by

$$\hat{x}(0|0) = \begin{pmatrix} 0 \\ 0 \\ 0 \end{pmatrix} \qquad P(0|0) = \begin{pmatrix} 20^2 & 0 & 0 \\ 0 & 50^2 & 0 \\ 0 & 0 & .05 \end{pmatrix}.$$

Fig. (4.6d) shows the estimated (as well as the original) boundary from application of this 3-state processor to the observation shown in Fig. (4.6b).

Experimental results for the known and unknown luminance cases showed minimal degradation of the estimated boundary obtained from the 3-state as opposed to the

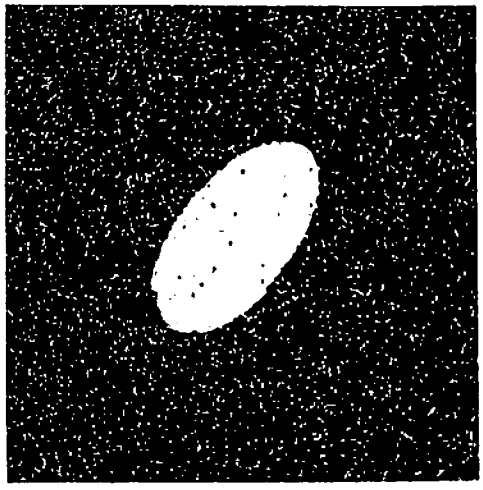

(a) Noisy ellipse, $\sigma = .5$

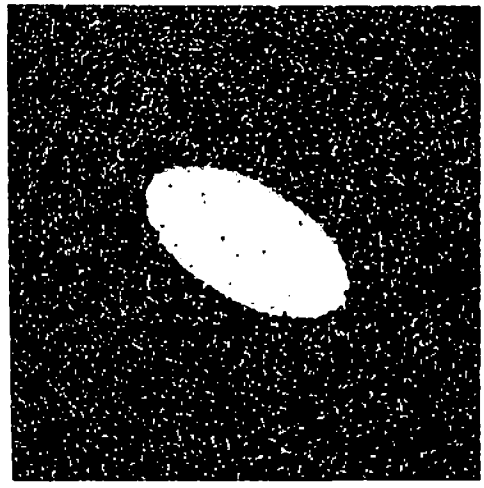

(b) Noisy ellipse, $\sigma = .5$

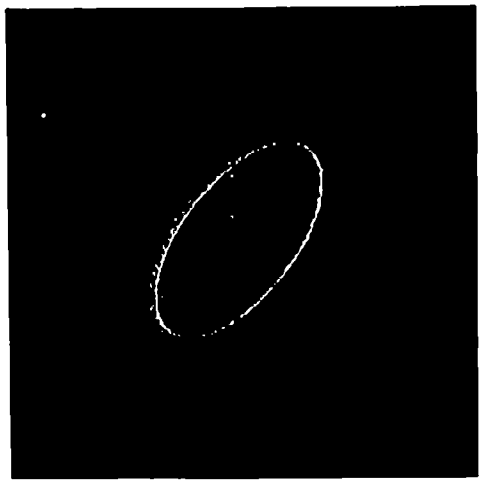

(c) Orig - est. boundaries, known intensities, 1, 0, 0

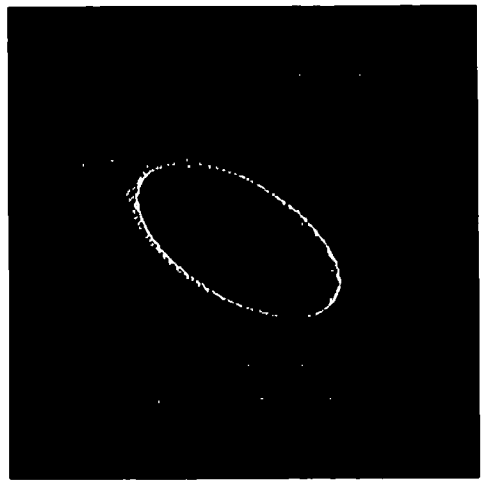

(d) Orig - est. boundaries, unknown intensities, 1, 0, 0

Fig. 4.6. Noisy ellipses and processor outputs with known and unknown object luminances.

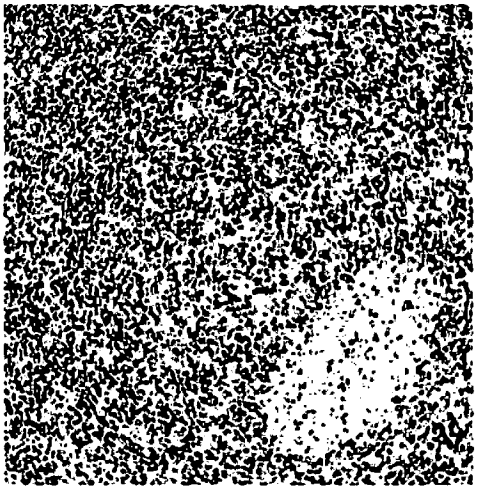

(a) Noisy ellipse, $\sigma = 2.0$

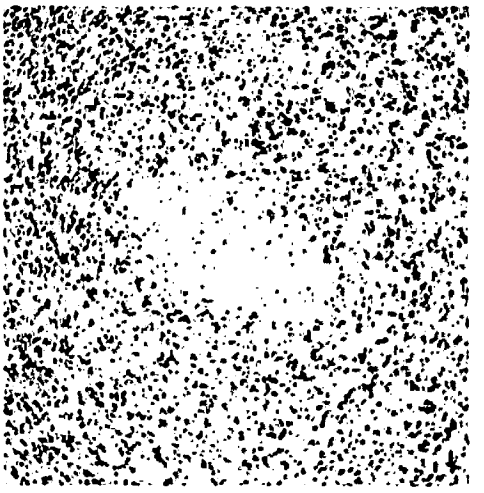

(b) Noisy ellipse, $\sigma = 3.0$

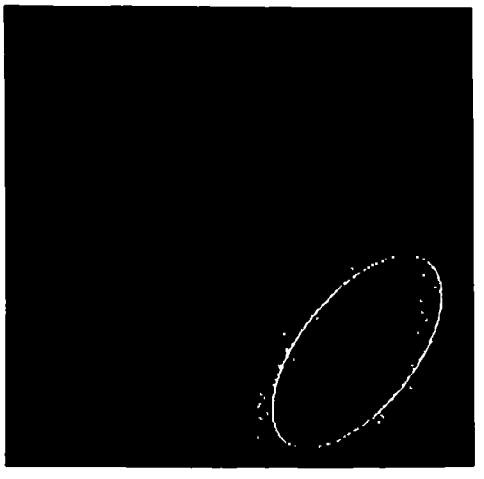

(c) Orig - est. boundaries, known intensities, 0, 1000, 1000

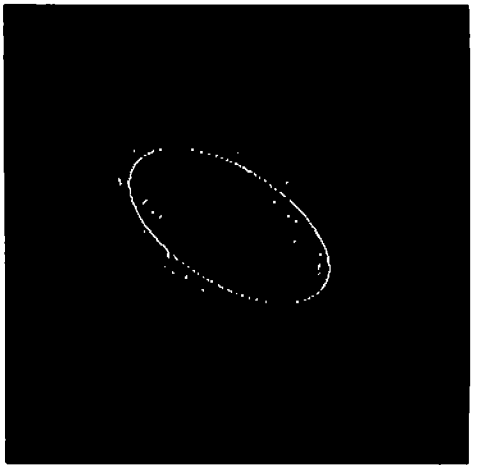

(d) Orig - est. boundaries, known intensities, 0, 800, 800

Fig. 4.7. Noisy ellipses ($\sigma = 2.0$ and $\sigma = 3.0$) and corresponding processor outputs.

2-state processor as can be appreciated by comparison of Figs. (4.6d) and (4.6c).

A different set of 256X256 pictures has also been used to test the boundary processor. The original image illustrated in Fig. (4.8a) with the histogram shown in Fig. (4.9), depicts an armored personnel carrier (APC) on a natural scene. This picture has been selected as an example of a realistic image and it is available from the data base of the University of Southern California [30]. To test the processor performance in textured environments, the APC picture has been assumed to represent a binary image.

Inspection of the histogram revealed two peaks that were chosen as the "constant" luminance values of the object and background (s_o=56, s_b=132). With the original an 8-bit image, the luminance values were linearly mapped into the interval [0,1] before addition of white Gaussian noise of standard deviation σ, to generate the set of observations appearing in Fig. (4.8b) and Figs. (4.10a,b). In displaying these observations, luminances above 1 were set to 1 and those below 0 as zero (equivalently 255 and 0).

The parameters for this processor, gathered by the procedures indicated previously when estimating the elliptical boundaries, were:

$$N = 256 \quad \bar{w} = 75.8 \quad \bar{c} = -4.6 \quad p_0 = .5 \quad p_1 = .5$$

$$S_o = .220 \quad S_b = .518$$

while the matrices $A_o(jN)=A_o$, $B_o(jN)=B_o$ and initial conditions $\hat{r}(0|0)$ and $P(0|0)$ corresponded to:

$$A_o = \begin{pmatrix} .876 & 0 \\ 0 & .924 \end{pmatrix} \qquad B_o = \begin{pmatrix} 4.02 & 0 \\ 0 & 2.12 \end{pmatrix}$$

$$\hat{r}(0|0) = \begin{pmatrix} 0 \\ 0 \end{pmatrix} \qquad P(0|0) = \begin{pmatrix} 150 & 0 \\ 0 & 200 \end{pmatrix}.$$

The results for three different noise levels appear in Figs. (4.8c,d) and Figs. (4.10c,d). In contrast to the pattern followed in Figs. (4.6,7) where the estimated as well as the original boundaries were shown in the same picture, only the estimated boundary is shown in Figs. (4.8,10), with the exception of Fig. (4.8c) where the original boundary (brighter trace) is also printed. Because the estimator provides at every line only the width and center values (equivalently, the initial and final pixels the object occupies on the line), to help in visualizing the APC boundary, all the pixels on the first and last lines belonging to the estimated object have been shown as part of the boundary too.

It must be pointed out: (1) from Fig. (4.8c) that although the processor has succesfully extracted the object in the picture, it has also identified the shadow on the left as belonging to the APC; this however, is not surprising in view of Fig. (4.8b) where even visual separation is difficult. (2)That though the noise variances for the ellipse cases were bigger, the luminance difference between background and foreground was greater too. (3) That a single processor was used, even though the ellipses were located in different positions and with different orientations. And (4) the applicability of the processor in cases of severe noise degradation.

Experimental Remarks: Under this heading several queries as well as answers will be considered. The answers are mainly observations born out of the experiments, and conclusions drawn are limited in this respect.

It was indicated that for the processor implemented before, the computation bulk was associated with the estimation stage.

Recall that for the estimator to proceed, it is necessary to establish first which one of the interceptions illustrated in Fig. (4.3) occurs. Two different ways to carry out this classification correspond to an enumeration or a general approach. In the second method, the interception is found from a set of tests that locate the

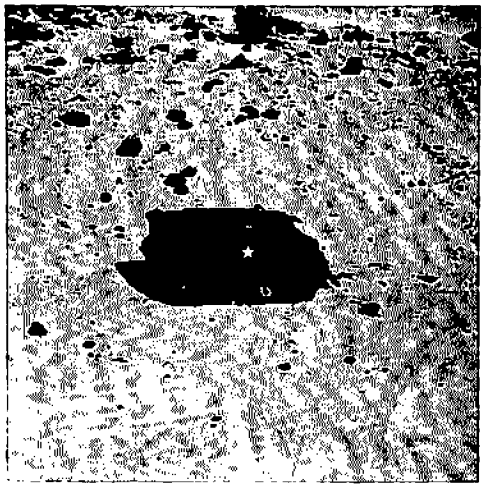

(a) APC original

(b) Noisy APC, $\sigma = .1$

(c) Original and estimated APC boundaries, known intensities, 1, 0, 0

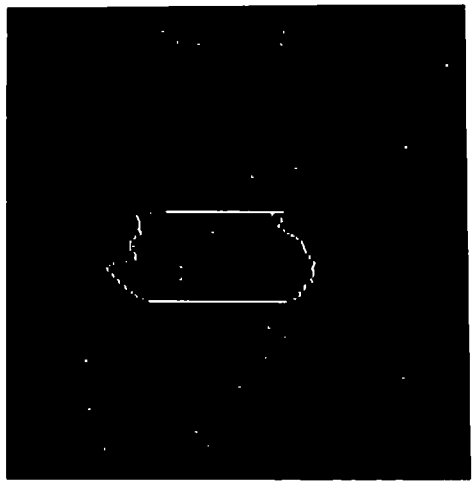

(d) Estimated APC boundary, known intensities, 1, 0, 0

Fig. 4.8. Original APC, noisy observation ($\sigma = .1$) and processor output.

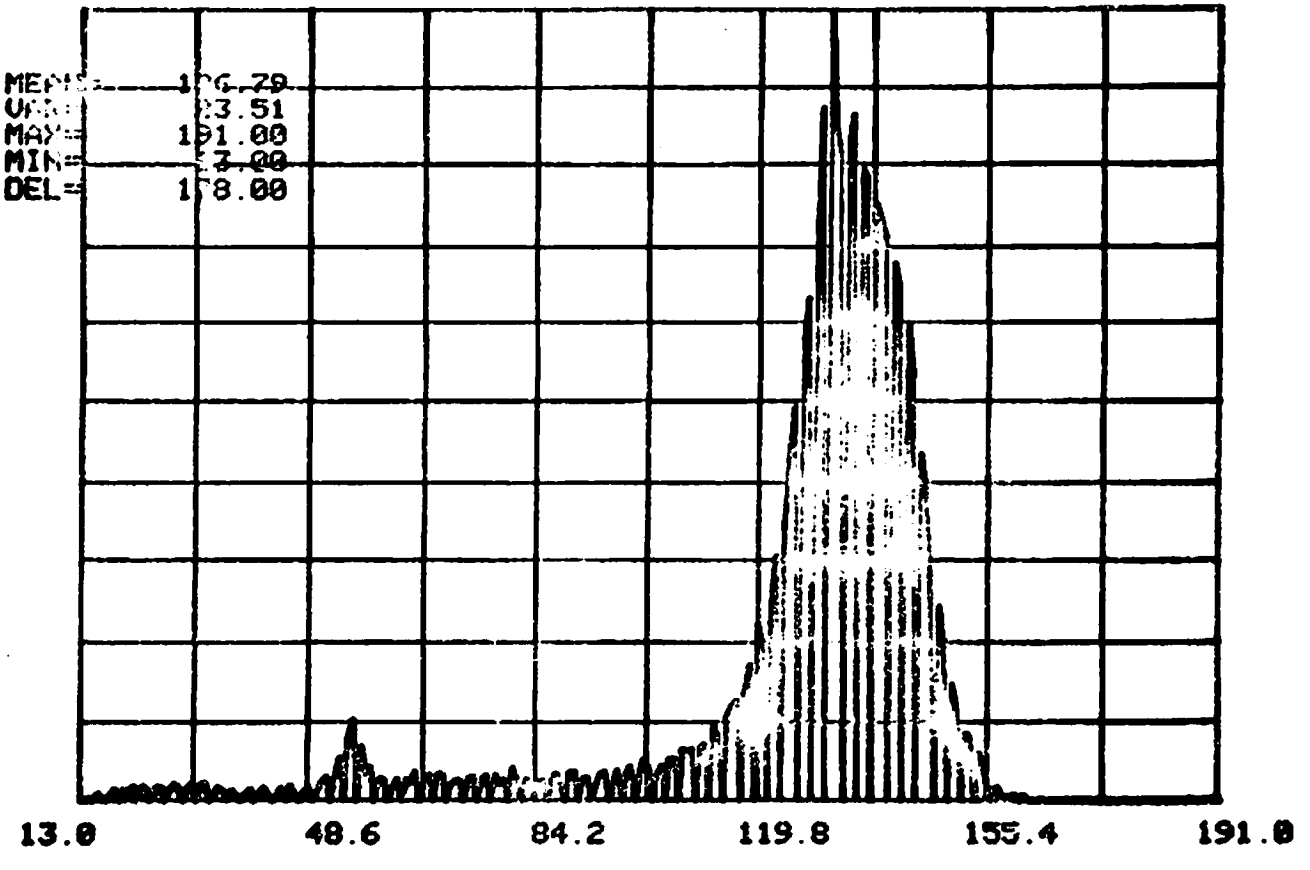

Fig. 4.9. APC histogram.

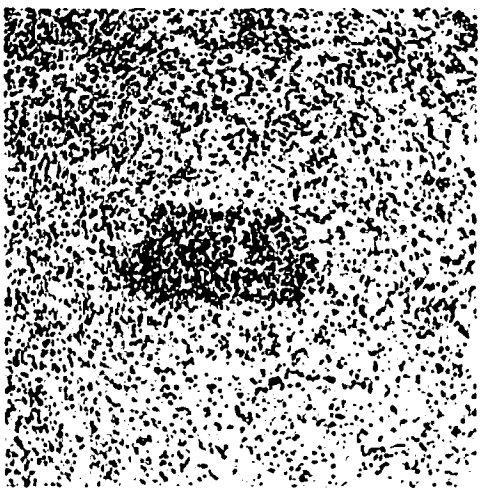

(a) Noisy APC, $\sigma = .6$

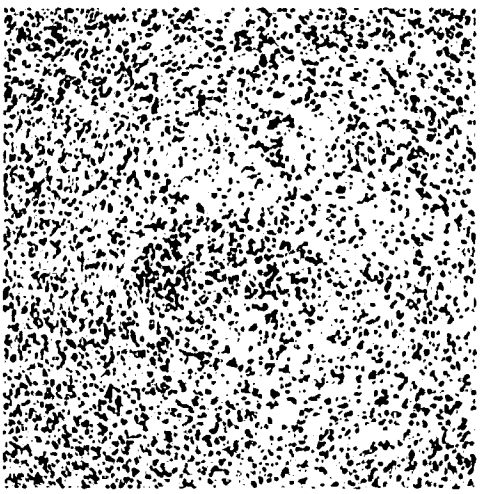

(b) Noisy APC, $\sigma = 1.2$

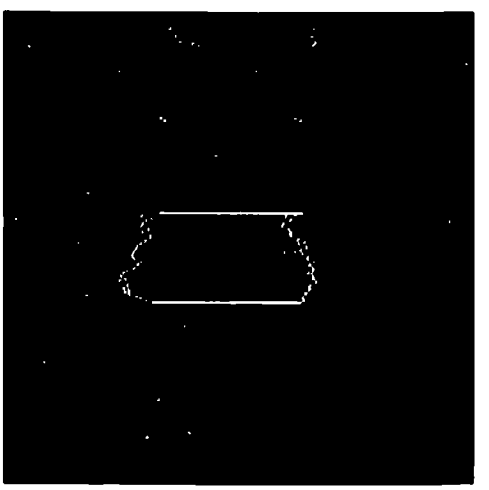

(c) Estimated APC boundary, known intensities, 1, 0, 0

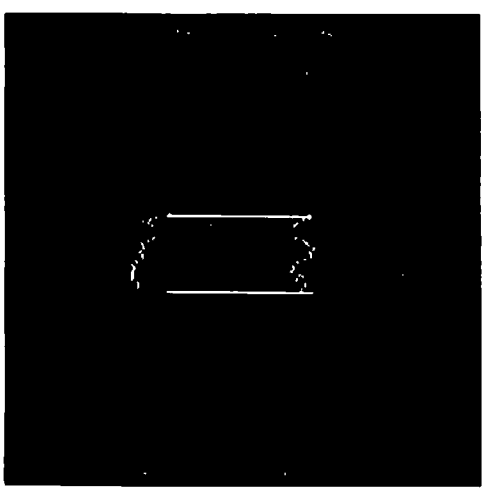

(d) Estimated APC boundary, known intensities, 0, 260, 260.

Fig. 4.10. Noisy APC ($\sigma = .6$ and $\sigma = 1.2$) and processor outputs.

vertices of the rectangular region (□) with respect to the boundary lines (Δ) derived from (2.10). This type of search was used in the preceding examples and it is appropriate when there is no indication as to how often the different interceptions occur. The enumeration approach, on the other hand, produces a search directed by the occurrence of the interceptions. Under this method, the search is designed to use a minimum number of tests to establish whether the most frequent interception has occurred. The other interceptions are tested in order of decreasing occurrence. Incidentally, it was observed while processing the APC pictures that approximately 99% of the interceptions corresponded to the one shown in Fig. (4.2). Hence, if applied in this instance, the enumeration approach should result in a faster algorithm.

Another way to speed up the estimator above, involves the use of a simplified algorithm. In this case, the search in Fig. (4.3) is eliminated. Instead, I-4 is assumed to happen at all times. This simplification can result in a poorer estimate depending on the frequency of appearance of the selected interception. Note that as long as the estimate error variances remain reasonably small, the region □ will be small in relation to Δ and consequently lie within it. On the other hand, large error variances will tend to correspond to the rest of the interceptions. Thus, when the variances are small, the

original as well as the simplified algorithms should result in very similar estimates. As the variances increase, the simplified algorithm should produce different estimates and larger variances. Hence, if it is true that larger variances indicate more uncertain estimates, the simplified estimator results in poorer estimates. On the processor level, however, the estimate can be accepted or rejected depending on a threshold that would be higher for bigger variances. This would imply a higher rejection rate from the detector. In summary, the simplified algorithm proposed, being faster than the original, while degrading poor estimates, produces negligible changes on estimates with small associated variances.

The cost values chosen depend on the particular processor application. As a result, only guidelines to make a selection can be given. Of course, it is known how the different costs affect qualitatively the resulting output. For example, the important quantities involved are $(c_{1,0} + f_{1,0} - c_{0,0})$, $(c_{0,1} - c_{1,1})$ and tr P^*. A first consideration to make deals with the relative values associated with non-detection and false alarming or for this matter, between $(c_{0,1} - c_{1,1})$ and $(c_{1,0} + f_{1,0} - c_{0,0})$. The second consideration refers to the various degrees of emphasis that can be applied on the estimation or the detection stages, depending on the numerical values assigned to the previous costs in relation to the

covariance trace. In finding an answer to the detection vs. estimation consideration it was found that under low noise conditions high penalties of detection were a good choice; this in turn corresponded to setting the variable threshold near 1 (zero if logarithms are used) when equal weights were put on either wrong detector decision. In noisier environments, however, the constant threshold detector proved to be useless. Under severe noise conditions, the covariance trace needs to be taken into consideration. Detection costs too high will produce poor estimates; costs too low will miss the object completely because the covariance term will raise the threshold too high. In general, it is convenient to start with low costs and raise them until satisfactory results are obtained.

This chapter concludes with the presentation in Fig. (4.11) of the flow chart for the boundary processor of binary images with known luminance values. The flow chart for unknown levels can be obtained by simple modifications of Fig. (4.11).

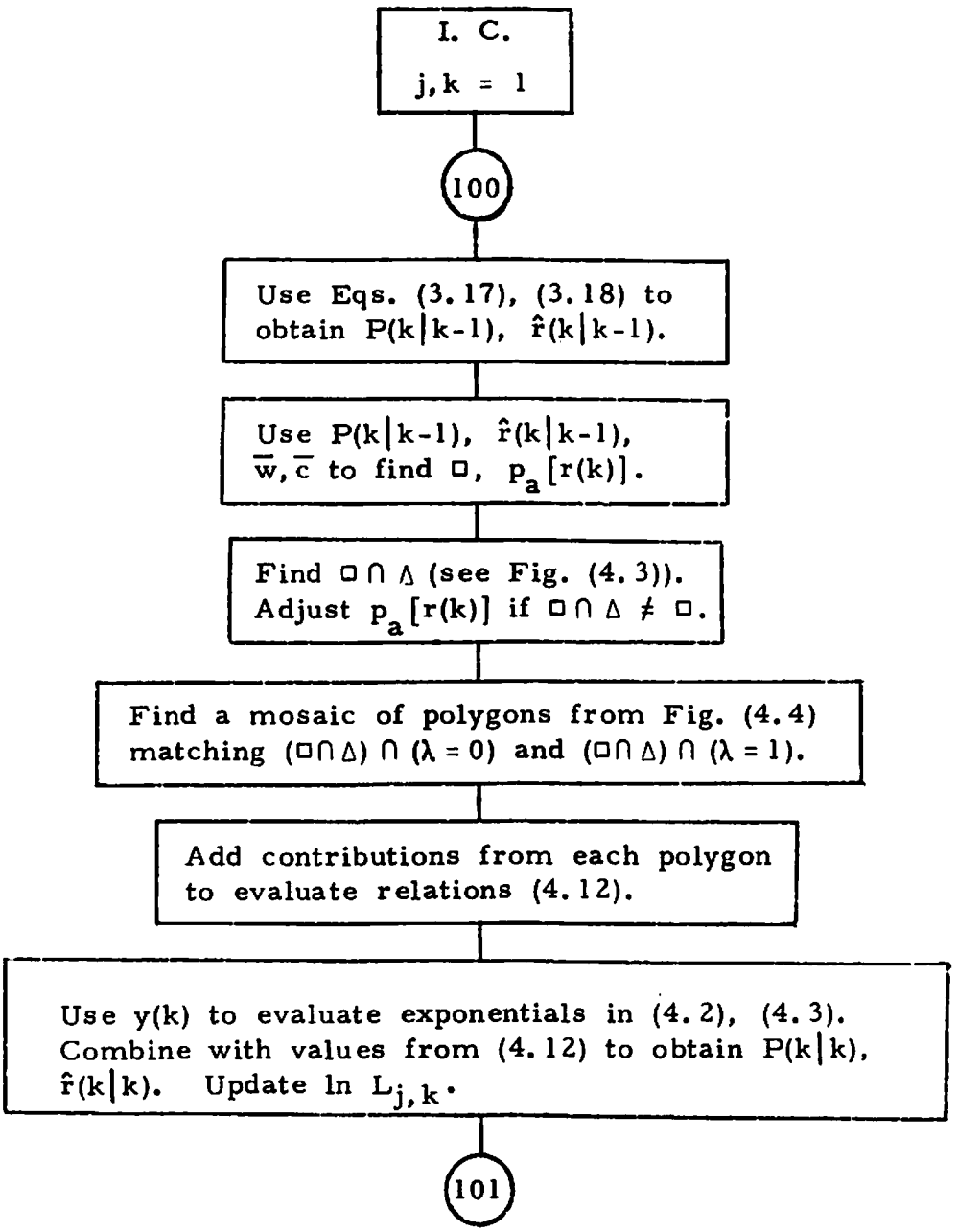

Fig. 4.11. Flow chart for boundary processor for binary images of known luminance.

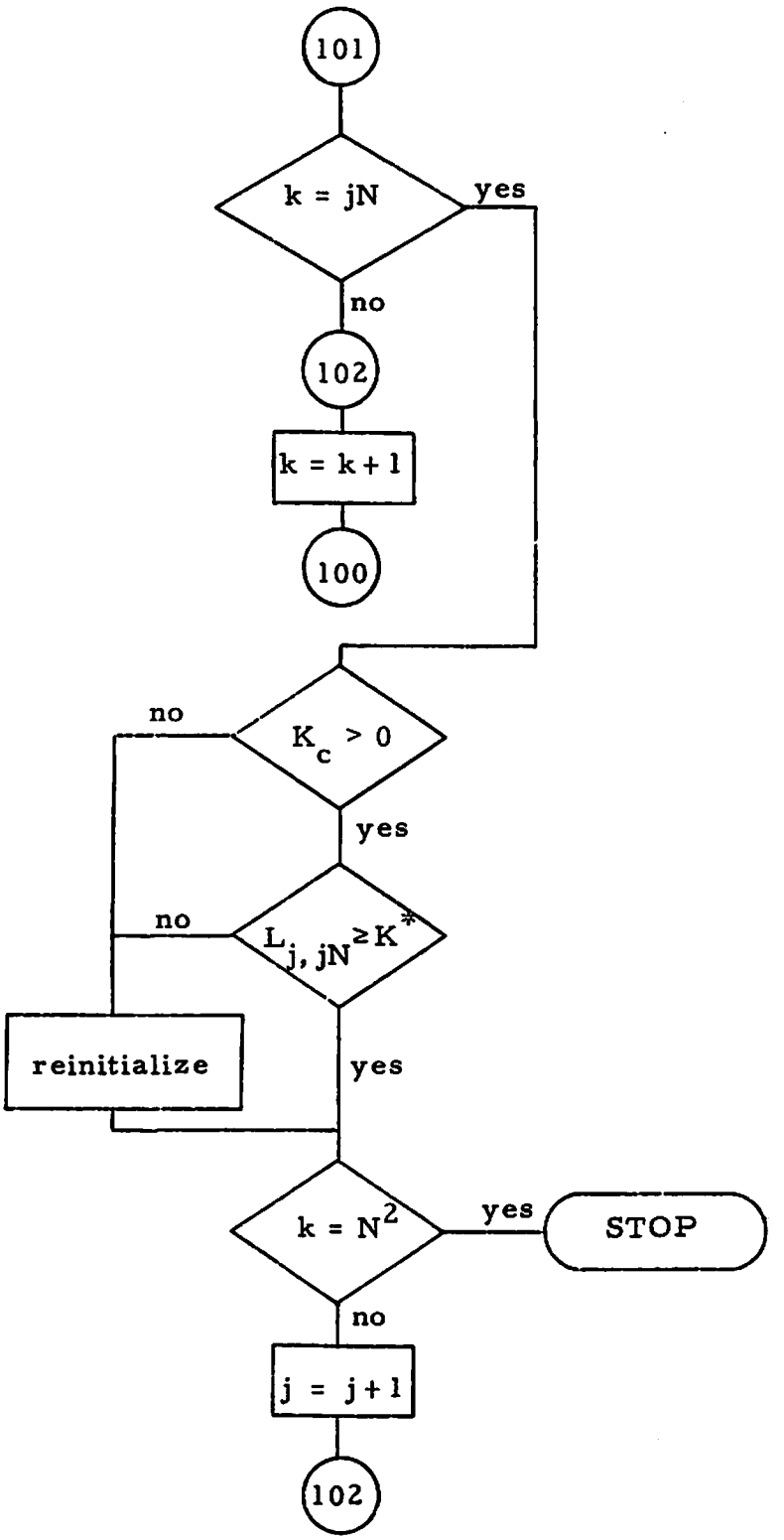

Fig. 4.11. Continued

CHAPTER FIVE

Conclusions, Comments and Further Work

A comparison between the processor derived in this work and the boundary estimator in [33] (see Fig. (5.1)) can now be made. It should be noted that both estimators are identical while the detectors are not. Two new elements are present in Fig. (5.1) that were not part of the processor in chapter three. The switch on the left closes after the line estimates are computed. The line storage is necessary for the detector to be able to use part of the observation sequence to make a decision after the estimates are available. The estimates in turn, serve to determine which part of the observation the detector will use and which part will be disregarded in performing the acceptance or rejection test. The subscript on the likelihood ratio (Λ_{est}) calculated in [33] as well as the arrow stemming from the estimator serve to point explicitly this dependence on the estimated values. The main disadvantage associated with this boundary estimator is the line storage required.

Other structures to perform boundary estimation in the context of joint detection and estimation can be proposed.

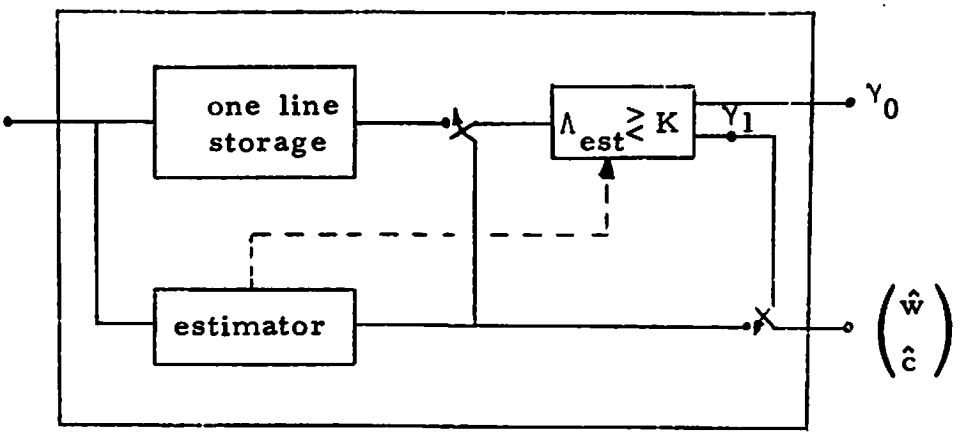

Fig. 5.1. Boundary processor in [33].

Fig. (5.2), for instance, illustrates a processor that uses a function of the observations at the detector imput. Letting

$$Y_s = Y_s(j) = \sum_{k=(j-1)N+1}^{jN} y(k) \quad . \qquad (5.1)$$

The joint cost of estimation and detection for some chosen cost function can be written as:

$$R_{D+E} = \int dY_s \{ \delta(\gamma_0 | Y_s)[p_0 c_{0,0} p(Y_s|H_0) + p_1 c_{0,1} p(Y_s|H_1)] + \delta(\gamma_1 | Y_s)[p_0(c_{1,0} + f_{1,0}) p(Y_s|H_0) + p_1 c_{1,1} p(Y_s|H_1)] + f_{1,1}(r_{est}, r)]\} \qquad (5.2)$$

where

$$f_{1,1}(r_{est}, r) = p_1[\int dr [r_{est} - r]'[r_{est} - r] p(r|Y, H_1)][\int dY\, p(Y|H_1)]$$

$$= p_1\, p(Y_s|H_1)[\int dr[r_{est} - r]'[r_{est} - r]\, p(r|Y, H_1)] \qquad (5.3)$$

where the integration in (5.3) on Y is performed over all Y such that (5.1) is satisfied.

The value of r_{est} minimizing (5.3) and consequently (for a fixed decision rule) (5.2), corresponds to:

$$r^*[jN|Y(j)] = E[r(jN)|Y(j), H_1] \qquad (5.4)$$

with

$$\text{tr } P^* = \int dr [r^* - r]'[r^* - r]\, p(r|Y, H_1) \quad .$$

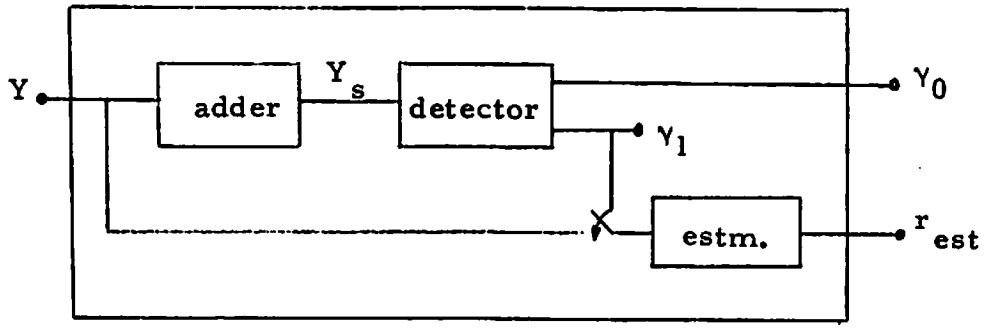

(a) Proposed processor

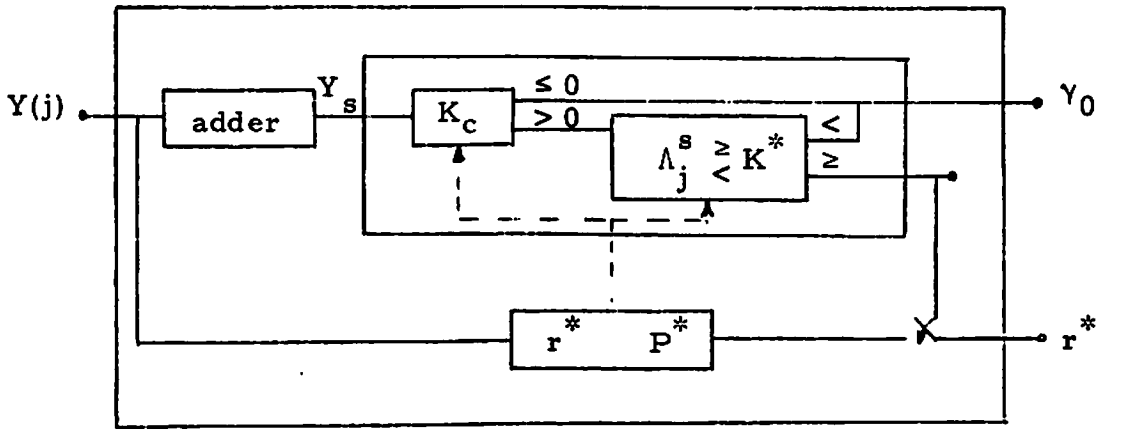

(b) Optimal processor

Fig. 5.2. A processor that inputs a function of the observations to the detector.

The optimal decision rule obtained after some simplification reduces to:

if $$c_{0,1} - (c_{1,1} + \text{tr } P^*) > 0 \qquad (5.5a)$$

then

$$\Lambda_j^s = \frac{P_1\, p(Y_s|H_1)}{P_0\, p(Y_s|H_0)} \begin{matrix} \gamma_1 \\ > \\ < \\ \gamma_0 \end{matrix} \frac{c_{1,0} + f_{1,0} - c_{0,0}}{c_{0,1} - (c_{1,1} + \text{tr } P^*)} \qquad (5.5b)$$

decide γ_0 if $c_{0,1} - (c_{1,1} + \text{tr } P^*) \leq 0$. (5.5c)

Notice in particular the very simple detector (no N-dimensional densities involved as was the case in chapter three). A processor of this type should be desirable in cases where the statistics of Y_s are directly available or are easy to obtain.

Let us indicate at this point, that the list of boundary processors cited throughout this work has by no means been an exhaustive enumeration. On the contrary, it is intended to awake the interest in this form of estimation and to express the need for a complete classification of processors in terms of cost functions, applications (uses), capabilities, advantages and disadvantages.

Let us refer to the two main restrictions imposed on the images: two-textured and horizontally convex objects.

Note first that, saying an image has two textures is not the same as saying it is a binary valued picture, i.e., zeros and ones. Indeed, the representation (1.6) has often been used in the past when dealing with monochrome multi-valued images [21,24,26,31], and it can be used to model each of the textures, when representing images by replacement processes. Viewed in this way, the model associated with (1.6) can be interpreted as a particular and degenerate case of the replacement formulation where only one texture is involved (it covers the entire picture). Hence, the fidelity achieved in representing images as composed of two or, by the same token, more textures is very dependent on the designer emphasizing complexity of texture model with reduced number of textures or simplicity in texture model but allowing additional textures to be present.

It is convenient to recall, that it is the horizontal convexity constraint which is the factor that reduces the problem of boundary determination to the estimation of only two parameters: w(k) and c(k). When this restriction does not apply, then it is necessary to redefine relations (2.9) appropriately. One way to proceed is to associate more than one pair of parameters to the replacement function λ. as many as required by the classes of objects investigated. e.g., for images containing objects like the one depicted in Fig. (2.2a) four parameters suffice. Clearly as the

number of parameter pairs increases, so does the processor size (total amount of computation). The case of multi-textured images is dealt with similarly. However, instead of associating several width and center pairs to the replacement function λ , now each λ_i , carries a pair (w_i, c_i) associated to it

A topic for future investigation consists in the computational requirements for images with textures modeled by dynamic systems of bigger dimensionality than those considered in the applications, i.e., $\leq$ 2. It is of considerable importance too, to establish the sensitivity of the algorithm to different densities $p_a[x(k)]$, and at the same time the available simplifications derived from the use of these densities.

Summary

A solution to the problem of boundary determination, an important topic in automated image understanding, has been presented. The images considered were composed of two textures (a horizontally convex object on a background) and were characterized statistically. An optimal boundary estimator has been derived by minimizing the average cost of joint detection and estimation for appropriately chosen cost functions.

Furthermore, in view of information restrictions, recursive easily implementable algorithms updating only first and second order moments were developed to carry out the tasks of estimation and detection. Applications to pictures of a military vehicle and computer generated objects have been presented. Finally, ways to relax the constraints were indicated as well as other types of possible candidate processors.

REFERENCES

[1] A. Rosenfeld and A. C. Kak, Digital Picture Processing, Academic Press, New York, 1976.

[2] L. S. Davis, A. Rosenfeld and J. S. Weszka, "Region Extraction by Averaging and Thresholding," IEEE Trans. on Systems, Man and Cybernetics, Vol. SMC-5, No. 3, May 1975, pp. 383-388.

[3] S. W. Zucker, A. Rosenfeld and L. S. Davis, "Picture Segmentation by Texture Discrimination," IEEE Trans. on Computers, Vol. C-24, No.12, Dec. 1975, pp. 1228-1233.

[4] L. G. Roberts, "Machine Perception of Three Dimensional Solids," Optical and Electro-Optical Information Processing, (J. Tippet, D. Berkowitz, L. Clapp, C. Koester, A. Vanderbugh, Eds.) M.I.T. Press, 1965, pp. 159-197.

[5] A. Rosenfeld and M. Thurston, "Edge and Curve Detection for Visual Scene Analysis," IEEE Trans. on Computers,Vol. C-20, No. 5, May 1971, pp. 562-569.

[6] A. Rosenfeld, "A Nonlinear Edge Detection Technique," Proc. IEEE (letters), Vol. 58, No. 5, May 1970, pp. 814-816.

[7] W. Frei and C. C. Chen, "A Study of Fast Boundary Detection Operators," IEEE Trans. on Computers (to appear).

[8] M. Hueckel, "An Operator Which Locates Edges in Digital Pictures," J. Assoc. Comput. Mach., Vol. 18, No. 1, January 1971,pp.113-125.

[9] M. Hueckel, "A Local Visual Operator Which Recognizes Edges and Lines," J. Assoc. Comput. Mach., Vol. 20, No. 4, Oct. 1973, pp. 634-647.

[10] A. K. Griffith, "Mathematical Models for Automatic Line Detection," J. Assoc. Comput. Mach., Vol. 20, No. 1, Jan. 1973, pp. 62-80.

[11] A. K. Griffith, "Edge Detection in Simple Scenes Using A Priori Information," IEEE Trans. on Computers, Vol. C-22, No. 4, April 1973, pp. 371-381.

[12] R. Nevatia, "Locating Object Boundaries in Textured Environments," IEEE Trans. on Computers, Vol. C-25, No. 11, Nov. 1976, pp. 1170-1175.

[13] R. Nevatia and K. Laws, "Extention of Boundary Segments in a Multi-Level System," USCIPI Report 740, University of Southern California, March 1977, pp. 29-34.

[14] R. Nevatia and P. Chuan, "Detection of Edges in Elongated Neighborhoods," USCIPI Report 740, University of Southern California, March 1977, pp. 34-38.

[15] J. R. Fram and E. S. Deutsch, "On the Quantitative Evaluation of Edge Detection Schemes and Their Comparison with Human Performance," IEEE Trans. on Computers, Vol. C-24, No. 6, June 1975, pp. 616-628.

[16] W. K. Pratt, "Figure of Merit for Edge Location," USCIPI Report 660, University of Southern California, March 1976, pp. 85-93.

[17] L. S. Davis, "A Survey of Edge Detection Techniques," Comput. Graph. Image Proc., Vol. 4, No. 3, Sep. 1975, pp. 248-270.

[18] M. D. Levine, "Feature Extraction: A Survey," Proc. IEEE, Vol. 57, No. 8, August 1969, pp. 1391-1407.

[19] D. N. Graham, "Image Transmission by Two-Dimensional Contour Coding," Proc. IEEE, Vol. 55, No. 3, March 1967, pp. 336-346.

[20] D. G. Lebedev and D. S. Lebedev, "Quantizing the Images by Separation and Quantization of Contours," Engrg. Cybernetics, No. 1, Jan.-Feb. 1965, pp. 77-81.

[21] L. E. Franks, "A Model for the Random Video Process," Bell System Tech. J., Vol. 45, No. 4, April 1966, pp. 609-630.

[22] N. E. Nahi and T. Assefi, "Bayesian Recursive Image Estimation," IEEE Trans. on Computers, Vol. C-21, No. 7, July 1972, pp. 734-738.

[23] N. E. Nahi, "Role of Recursive Estimation in Statistical Image Enhancement," Proc. IEEE, Vol. 60, No. 7, July 1972, pp. 872-877.

[24] A. O. Aboutalib and L. M. Silverman, "Restoration of Motion Degraded Images," IEEE Trans. on Circuits and Systems, Vol. CAS-22, No. 3, March 1975, pp. 278-286.

[25] N. E. Nahi and C. A. Franco, "Recursive Image Enhancement-Vector Processing," IEEE Trans. on Communications, Vol. COM-21, No. 4, April 1973, pp. 305-311.

[26] C. A. Franco, "Recursive Image Estimation," Ph.D. Dissertation, Dep. Elec. Eng., Univ. Southern California, Los Angeles, Feb. 1973.

[27] W. K. Pratt, "Generalized Wiener Filter Computation Techniques," IEEE Trans. on Computers, Vol. C-21, No. 7, July 1972, pp. 636-641.

[28] W. K. Pratt and F. Davarian, "Fast Computational Techniques for Pseudoinverse and Wiener Image Restoration," IEEE Trans. on Computers, Vol. C-26, No. 6, June 1977 (to appear).

[29] M. Jahanshahi, Statistical Scene Analysis: Boundary Estimation of Objects in Presence of Noise, USCIPI Report 590, University of Southern California, August 1975.

[30] N. E. Nahi, "Image Modeling by Replacement Processes," Proc. of the Symposium on Current Mathematical Problems in Image Science, Monterey, California, Nov. 1976.

[31] A. Habibi, "Two-Dimensional Bayesian Estimate of Images," Proc. IEEE, Vol. 60, No. 7, July 1972, pp. 878-883.

[32] N. E. Nahi and A. Habibi, " Decision Directed Recursive Image Enhancement," IEEE Trans. on Circuits and Systems, Vol. CAS-22, No. 3, March 1975, pp. 286-293.

[33] N. E. Nahi and S. Lopez-Mora, "Estimation of Object Boundaries," Proc. of the 1976 IEEE Decision and Control Conference, Clearwater, Florida, Dec. 1976, pp. 607-612.

[34] W. R. Bennett, "Statistics of Regenerative Digital Transmission," Bell System Tech. j., Vol. 33, No. 6, Nov. 1958, pp. 1501-1542.

[35] W. A. Gardner and L. E. Franks, "Characterization of Cyclo-Stationary Random Signal Processes," IEEE Trans. Inform. Theory, Vol. IT-21, No. 1, Jan. 1975, pp. 4-14.

[36] R. L. Kashyap and A. R. Rao, Dynamic Stochastic Models from Empirical Data, Academic Press, New York, 1976.

[37] E. Wong, "A Likelihood Ratio Formula for Two-Dimensional Random Fields," IEEE Trans. Inform. Theory, Vol. IT-20, No. 4, July 1974, pp. 418-422.

[38] E. Wong, "Detection and Filtering for Two-Dimensional Fields," Proc. of the 1976 Decision and Control Conference, Clearwater, Florida, Dec. 1976, pp. 591-595.

[39] D. Middleton and R. Esposito, "Simultaneous Optimum Detection and Estimation of Signals in Noise," IEEE Trans. Inform. Theory, Vol. IT-14, No. 3, May 1968, pp. 434-444.

[40] A. Fredriksen, D. Middleton and D. Vandelinde, "Simultaneous Signal Detection and Estimation under Multiple Hypotheses," IEEE Trans. Inform. Theory, IT-18, No. 5, Sept. 1972, pp. 607-614.

[41] N. E. Nahi, "Optimum Recursive Estimation with Uncertain Observation," IEEE Trans. Inform. Theory, Vol. IT-15, No.4, July 1969, pp. 457-462.

[42] A. G. Jaffer and S. C. Gupta, "Recursive Bayesian Estimation with Uncertain Observation," IEEE Trans. Inform. Theory, Vol. IT-17, No. 5, Sept. 1971, pp. 614-616.

[43] A. G. Jaffer and S. C. Gupta, "Coupled Detection-Estimation of Gaussian Processes in Gaussian Noise," IEEE Trans. Inform. Theory, Vol. IT-18, No. 1, Jan. 1972, pp. 106-110.

[44] M. D. Srinath and P. K. Rajasekaran, "Estimation of Randomly Occuring Stochastic Signals in Gaussian Noise," IEEE Trans. Inform. Theory, Vol. IT-11, No. 2, March 1971, p. 206.

[45] D. W. Kelsey and A. H. Haddad, "Detection and Prediction of a Stochastic Process Having Multiple Hypotheses," Inform. Sciences, Vol. 6, No. 4, Oct. 1973, pp. 301-311.

[46] D. W. Kelsey and A. H. Haddad, "A Note on Detectors for Joint Minimax Detection-Estimation Schemes," IEEE Trans. Autom. Control, Vol. AC-18 No. 5, Oct 1973, pp. 558-559.

[47] N. E. Nahi, Estimation Theory and Applications, R. E. Krieger Publishing Co., Huntington, New York, 1976.

[48] M. Athans, R. P. Wishner and A. Bertolini, "Suboptimal State Estimation for Continuous-Time Nonlinear Systems from Discrete Noisy Measurements," IEEE Trans. Autom. Control, Vol. AC-13, No. 5, Oct. 1968, pp. 504-514.

[49] L. Meier, "The Third Order Extended Kalman Filter," Proc. of the Symposium on Nonlinear Estimation Theory and Its Applications, San Diego, Cal., 1971, pp. 213-216.

[50] A. P. Sage and J. L. Melsa, Estimation Theory with Applications to Communications and Control, McGraw-Hill, New York, 1971.

[51] H. L. Van Trees, Detection, Estimation and Modulation Theory, Part I, John Wiley & Sons, New York, 1968.

[52] F. C. Schweppe, "Evaluation of Likelihood Functions for Gaussian Signals," IEEE Trans. Inform. Theory, Vol. IT-11, No. 1, Jan. 1965, pp. 61-70.

[53] T. Kailath, "A General Likelihood-Ratio Formula for Random Signals in Gaussian Noise," IEEE Trans. Inform. Theory, Vol. IT-15, No. 3, May 1969, pp. 350-361.

[54] T. Kailath, "A Further Note on a General Likelihood Formula for Random Signals in Gaussian Noise," IEEE Trans. Inform. Theory, Vol. IT-16, No. 4, July 1970, pp. 393-396.

[55] T. Kailath, "Likelihood Ratios for Gaussian Processes," IEEE Trans. Inform. Theory, Vol. IT-11, No. 3, May 1970, pp. 276-288.

[56] R. Esposito, "On a Relation Between Detection and Estimation in Decision Theory," Information and Control, Vol. 12, No. 2, Feb. 1968, pp. 116-120.

[57] T. Kailath, "A Note on Least-Squares Estimates from Likelihood Ratios," Information and Control, Vol. 13, No. 6, Dec. 1968, pp. 534-540.

[58] A. G. Jaffer and S. C. Gupta, "On Relations Between Detection and Estimation of Discrete Time Processes," Information and Control, Vol. 20, No. 1, Feb. 1972, pp. 46-54.

[59] A. G. Jaffer, "A Note on Conditional Moments of Randon Signals in Gaussian Noise," IEEE Trans. Inform. Theory, Vol. IT-18, No. 4, July 1972, pp. 513-514.

[60] L. L. Scharf and L. W. Nolte, "Likelihood Ratios for Sequential Hypothesis Testing on Markov Sequences," IEEE Trans. Inform. Theory, Vol. IT-23, No. 1, Jan. 1977, pp. 101-109.

[61] S. C. Schwartz, "Conditional Mean Estimates and Bayesian Hypothesis Testing," IEEE Trans. Inform. Theory, Vol. IT-21, No. 6, Nov. 1975, pp. 663-665.

[62] S. C. Schwartz, "The Estimator-Correlator for Discrete-Time Problems," IEEE Trans. Inform. Theory, Vol. IT-23, No. 1, Jan. 1977, pp. 93-100.

[63] J. R. McLendon and A. P. Sage, "Computational Algorithms for Discrete Detection and Likelihood Ratio Computation," Information Sciences, Vol. 2, No. 3, July 1970, pp. 273-298.

[64] C. R. Rao, Linear Statistical Inference and Its Applications, John Wiley & Sons, New York, 1973.

[65] R. Schmidt, The USC-Image Processing Institute Data Base, USCIPI Report 710, University of Southern California, Oct. 1976.

[66] D. G. Lainiotis, "On a General Relationship Between Estimation, Detection, And the Bhattacharyya coefficient," IEEE Trans. Inform. Theory, Vol. IT-15, No. 4, July 1969, pp. 504-505.

APPENDIX A

For illustrative purposes and to serve as a comparison with the quadratic error cost boundary processor, two additional problems involving simultaneous detection and estimation are considered in the following. The set of observations is assumed to be[1]

$$H_0 : y(k) = v(k)$$
$$H_1 : y(k) = s(k) + v(k) \qquad (A.1)$$

with s(k) representing a known signal dependent on a parameter r that needs to be estimated from the set of observations k=1,...,N. It is also assumed that all necessary statistics are known and available. Of particular interest are the processor structures.

Case 1: Let the set of costs be given by:

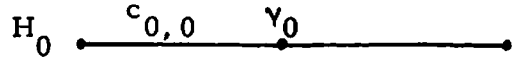

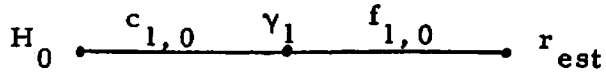

(1) To facilitate the comparison, most of the symbols used in the appendix and the main text are identical. There can be slight differences in meaning though.

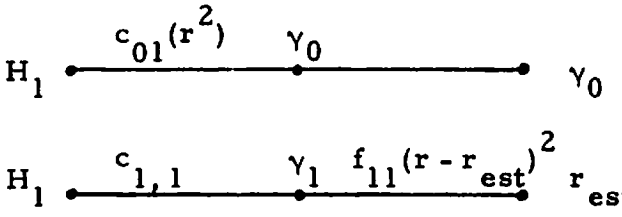

The average cost of joint detection and estimation R_{D+E} corresponds to:

$$
\begin{aligned}
R_{D+E} = \int dY \{ & \delta(\gamma_0|Y)[p_0\, c_{0,0}\, p(Y|H_0)] \\
& + \delta(\gamma_0|Y)[p_1\, c_{01} < r' r\, p(Y|r,H_1) > r \\
& + \delta(\gamma_1|Y)\, p_0[c_{1,0} + f_{1,0}]\, p(Y|H_0) \\
& + \delta(\gamma_1|Y)\, p_1 < [c_{1,1} + f_{11}(r - r_{est})'(r - r_{est}) \\
& \quad p(Y|r,H_1) > r\} \quad .
\end{aligned}
\tag{A.2}
$$

Hence,

$$
\begin{aligned}
R_{d+e} = & \delta(\gamma_0|Y)\, \{p_0\, c_{0,0}\, p(Y|H_0) \\
& + p_1\, c_{01} < r' r\, p(Y|r,H_1) > r\} \\
& + \delta(\gamma_1|Y)\, \{p_0(c_{1,0} + f_{1,0})\, p(Y|H_0) \\
& + p_1 < [c_{1,1} + f_{11}(r - r_{est})'(r - r_{est})]\, p(Y|H_1) > r\} \quad .
\end{aligned}
\tag{A.3}
$$

Using on (A.3) the same procedure applied to obtain (3.4) from (3.2), it follows that:

$$r^*[N|Y] = E[r(N)|Y, H_1] \qquad (A.4)$$

while the optimal decision rule δ^* becomes:

$$\delta^*(\gamma_0|Y) = 0 \quad , \quad \delta^*(\gamma_1|Y) = 1$$

if

$$p_0(c_{1,0} + f_{1,0})\, p(Y|H_0) + p_1(c_{1,1} + f_{11}\ \mathrm{tr}\ P^*)$$

$$p(Y|H_1) \leq p_0\, c_{0,0}\, p(Y|H_0) + p_1\, c_{01} < r'r$$

$$p(Y|r, H_1) > r = p_0\, c_{0,0}\, p(Y|H_0) +$$

$$p_1\, c_{01}(r^{*'} r^* + \mathrm{tr}\ P^*)\, p(Y|H_1) .$$

Collecting terms,

$$p_0(c_{1,0} + f_{1,0} - c_{0,0})\, p(Y|H_0) \leq$$

$$p_1[c_{01}(r^{*'} r^* + \mathrm{tr}\ P^*) - (c_{1,1} + f_{11}\ \mathrm{tr}\ P^*)]\, p(Y|H_1) \quad .$$

Therefore, the optimal detector decisions are:

$$\left.\begin{aligned} \delta^*(\gamma_1|Y) &= 1 \\ \delta^*(\gamma_0|Y) &= 0 \end{aligned}\right\} \quad \text{if} \quad \left\{\begin{aligned} &K_c > 0 \\ &\text{and} \\ &\Lambda_N \geq K^* \end{aligned}\right. \qquad (A.5)$$

$$\left.\begin{aligned}\delta^*(\gamma_0|Y) &= 1\\ \delta^*(\gamma_1|Y) &= 0\end{aligned}\right\} \quad \text{if} \quad \left\{\begin{array}{l} K_c \le 0 \\ \text{or} \\ \left\{\begin{array}{l} K_c > 0 \\ \text{and} \\ \Lambda_N < K^* \end{array}\right. \end{array}\right. \qquad (A.6)$$

where,

$$K_c = c_{01}\, r^{*'}\, r^* - c_{1,1} + (c_{01} - f_{11})\, \mathrm{tr}\, P^*$$

$$K^* = (c_{1,0} + f_{1,0} - c_{0,0})/K_c$$

$$\Lambda_N = \frac{p_1\, p(Y|H_1)}{p_0\, p(Y|H_0)} \quad . \qquad (A.7)$$

Consequently, the processor above has the structure indicated in Fig. (3.2), the estimator being identical to that in (3.7) while the detector, although defined from relations equivalent to (3.2), (3.13) differs in the definition of K_c.

Case 2: A cost function appropriate for estimating energy-type parameters is the following:

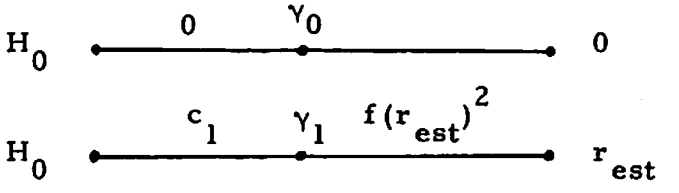

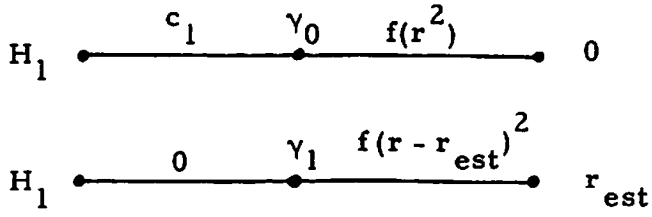

(A.8)

The set of observations is as given in (A.1). In this instance, wrong detection decisions are penalized c_1, but no cost is incurred if the decisions are correct. Two possible estimates are presented at the processor output: when the detector decides on γ_0, an estimate of zero is produced; otherwise, r_{est} is outputed. The processor is illustrated in Fig. (A1). Proceeding as in Case 1:

$$R_{D+E} = \int dY \{\delta(\gamma_0|Y)\, p_1 < (c_1 + f\, r'\, r)\, p(Y|r, H_1) > r$$

$$+ \delta(\gamma_1|Y)\, p_0 (c_1 + f\, r'_{est}\, r_{est})\, p(Y|H_0) \qquad (A.9)$$

$$+ \delta(\gamma_1|Y)\, p_1\, f < (r - r_{est})'(r - r_{est})\, p(Y|r, H_1) > r\} .$$

Minimization of R_{D+E} is equivalent to minimizing R_{d+e}:

$$R_{d+e} = \delta(\gamma_0|Y)\{p_1 < (c_1 + f\, r'\, r)\, p(Y|r, H_1) > r\}$$

$$+ \delta(\gamma_1|Y)\{p_0\, c_1\, p(Y|H_0)\}$$

$$+ \delta(\gamma_1|Y)\, f\{p_0\, r'_{est}\, r_{est}\, p(Y|H_0)$$

$$+ p_1 < (r - r_{est})'(r - r_{est})\, p(Y|r, H_1) > r\} . \qquad (A.10)$$

In (A.10) only the terms inside the last braces depend on r_{est}. Hence, assuming a fixed decision rule, R_{d+e} is minimized by choosing r_{est} equal to:

$$r^*[N|Y] = \frac{\Lambda_N}{\Lambda_N + 1} \; E[r(N)|Y, H_1] \; . \qquad (A.11)$$

With Λ_N as in (A.7). Replacing r_{est} in (A.10) by r^* from (A.11), the optimal decision rule follows:

decide γ_1 if:

$$p_0 \, c_1 \, p(Y|H_0) + f\{p_0 \, r^{*'} \, r^* \, p(Y|H_0)$$

$$+ \, p_1 < (r - r^*)'(r - r^*) \, p(Y|r, H_1) > r\}$$

$$\leq p_1 < (c_1 + f \, r'r) \, p(Y|r, H_1) > r \; .$$

Which can be rearranged as:

$$\left.\begin{aligned} \delta^*(\gamma_1|Y) &= 1 \\ \delta^*(\gamma_0|Y) &= 0 \end{aligned}\right\} \quad \text{if} \quad \Lambda_N \geq K_{r_1^*} \qquad (A.12)$$

and

$$\left.\begin{aligned} \delta^*(\gamma_0|Y) &= 1 \\ \delta^*(\gamma_1|Y) &= 0 \end{aligned}\right\} \quad \text{if} \quad \Lambda_N < K_{r_1^*} \qquad (A.13)$$

where

$$r_1^* = E[\, r(N)|Y, H_1 \,] \qquad (A.14)$$

$$K_{r_1^*} = \sqrt{\frac{c_1}{c_1 + f r_1^{*\prime} r_1^*}} \qquad (A.15)$$

This optimal processor is illustrated in Fig. (A2). Note that (A.14) and (A.4) correspond to the same estimator, but (A.11) is only a fraction of the estimator (A.14). This fraction being equal to the a posteriori probability of occurence of hypothesis H given the set of observations [66]. Some other cost functions have been considered in [39,40,43]; although the estimators have the form in (A.11), the detector relations are much more complicated.

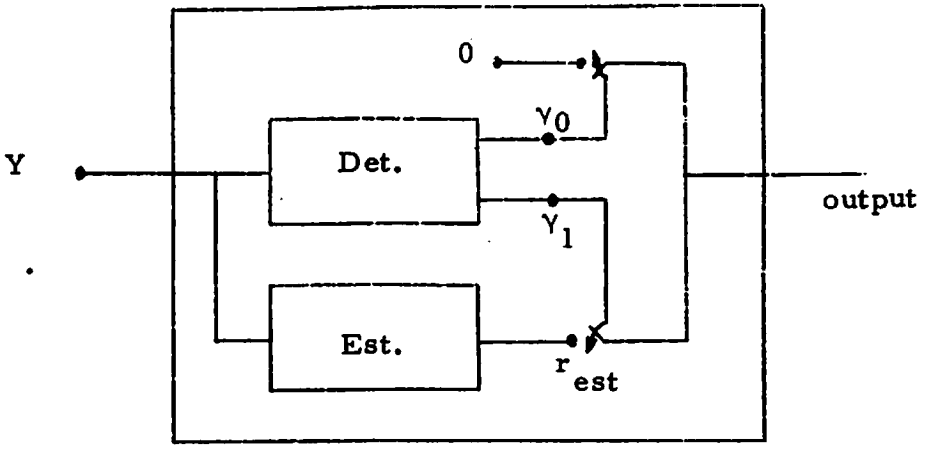

Fig. A1. Processor for case 1 (energy-type).

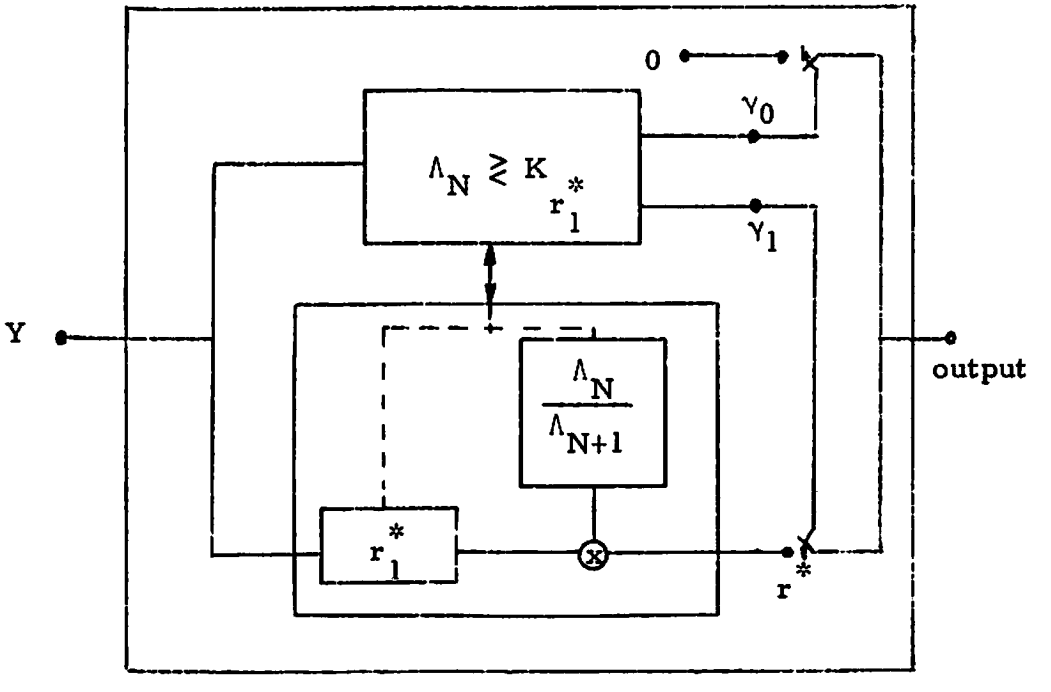

Fig. A2. Optimal processor for case 2.